Politecnico di Torino

Politecnico di Torino

Corso di Laurea in Ingegneria Energetica e Nucleare
A.a. 2021/2022
Sessione di Laurea Luglio 2022

Production of hydrogen from biogas:

Study, analysis of performance and production costs compared to traditional and innovative methods

Relatore:
Marta Gandiglio

Candidato:
Francesco Arena

Acknowledgements

First of all, I would like to thank Professor Marta Gandiglio, who gave me the opportunity to do this work, which helped to increase my interest in hydrogen production and the future opportunities related to this energy vector. I would like to thank the Professor for helping me during the work, especially in the parts that were most critical for me, and for sharing her knowledge with me. I prefer to write the next part in Italian so that it will be more understandable for the people to which I dedicate my thoughts.
Ringrazio tutti i miei amici conosciuti durante questo percorso a Torino con i quali abbiamo condiviso tanto e passato bellissimi momenti, in particolare Nick, Fra, Matti, Poul, Sacche, Jack, Michael.
Ringrazio gli amici di una vita, sempre vicini. Mauro, Emilio, Peppe, Santoro e tutti i ragazzi di Noepoli.
Ringrazio Alex e Giorgio, per me dei veri e propri fratelli, confidenti ed amici. Ci siamo sempre supportati e se sono qui adesso a scrivere queste parole in questo lavoro è anche grazie a voi.
Ringrazio mio fratello maggiore Flaminio, colonna portante, insostituibile, della mia vita.
Ed infine i miei genitori ai quali dedico questo lavoro. A voi che ci siete sempre, che mi sostenete, che illuminate le mie giornate e rendete semplici i momenti più difficili. Vi ringrazio per la forza ed il sapere che diffondete, quotidianamente, nel mio animo e per tutto quello che quotidianamente fate per me.

Abstract

The interest in finding strategies to decarbonise industrial processes and economic sectors where reducing carbon emissions is most difficult has meant that interest in hydrogen has grown rapidly in recent years in Europe and around the world. Hydrogen can be used as a raw material, fuel, carrier or energy storage and when used, it does not emit CO_2.

These characteristics mean that hydrogen can represent an alternative in the transport sector and also as an alternative in the natural gas grid. The most widely used technology for producing hydrogen to date is natural gas reforming (SMR), i.e. hydrogen produced in its 'grey' form, as this technology involves carbon dioxide emissions. For this reason, studies are converging towards production methods that have a completely renewable origin or by exploiting processes powered by energy from renewable sources, producing so-called 'green' hydrogen [1].

And it is precisely in this context that this study can be placed, as it analyses the process of producing hydrogen from biogas, produced through anaerobic digestion, by steam reforminig. The biogas taken into consideration derives from the wastewater treatment plant (WWTP) located in the city of Collegno (TO) from which annual production data were obtained and from these the average flow rate of biogas produced in a year of operation was calculated. This flow rate of 59.05 kg/h feeds the BSR plant, which was analysed using the Aspen Plus software. The basic design envisages a reforming temperature of 900 °C and allows the production of 8 kg/h of hydrogen, the plant was assumed to operate all year round allowing the production of 70080 kg of H_2/y. Following this, a sensitivity analysis was conducted on different reforming temperatures of 850° °C, 800°C, 750 °C, 700 °C. The most important results such as energy spent to produce 1 kg of H_2 , energy yield of the process and energy consumed by the plant were compared. The next analysis was to conduct a pinch analysis on the various processes using the Aspen Energy Analyzer V10 software, calculating the minimum heat to be supplied and the heat recoverable from the process. A heat exchanger network was then proposed for each process. Finally, the economic analysis of the process was assessed by evaluating the levelised cost of hydrogen (LCOH) and this was then compared with the prices for processes using electrolysis.

"Tutto è energia e questo è tutto quello che esiste. Sintonizzati alla frequenza della realtà che desideri e non potrai fare a meno di ottenere quella realtà. Non c'è altra via. Questa non è filosofia, questa è fisica."
[ALBERT EINSTEIN]

List of Figures

List of Tables

Contents

List of Acronyms

AD	Anerobic digestion
AEL	Alkaline electrolyzer
BEC	Bare Erected Cost
BG	Biogas
BSR	Biogas steam reforming
CAPEX	Capital expenditure
CEPCI	Chemical Engineering Plant Cost Index
CF	Capacity factor
EA	Energy activation
EPA	United States Environmental Protection Agency
EPCC	Engineering, Procurement and Construction Cost
GHG	Greenhouse gases
HEN	Heat exchanger network
HTWGS	Hot temperature water gas shift
IEA	International Energy Agency
LCOH	Levelized cost of hydrogen
LHV	Lower Heating Value
LTWGS	Low temperature water gas shift
MSW	Municipal solid waste
NETL	National Energy Technology Laboratory
OFMSW	Organic solid fraction of municipal solid waste
OM	Operation and maintenance
OPEX	Operating expenditure
PEM	Proton exchange membrane
PRMHV2	Peng Robinson state equations modified with Huron-Vidal mixing rule
PSA	Pressure swing adsorption
PSRK	Predictive Soave Redlich Kwong
PtH	Power to hydrogen
PtG	Power to gas
PV	Photovoltaic

ROE	Return on equity
SDS	Sustainable development scenario
SOE	Solid oxide cell
SOEC	Solid oxide electrolysis cell
SMR	Steam reforming
STEPS	Stated policy scenario
TASC	Total as spent capital
TOC	Total overnight capital
TPC	Total plant cost
VFA	Volatile fatty acid
WEO	World energy outlook
WGS	Water gas shift
WWTP	Wastewater treatment plant

Chapter 1

Introduction

Energy is one of the fundamental aspects of a country's development and economic growth. Nowadays, energy production is still dominated by processes that use fossil fuels, with the associated negative consequences caused by the use of such raw materials, such as, and above all, the production of CO_2,

For this reason, we are seeing policies globally push for greater use of renewable fuels and the development of technologies for the use of these energy carriers. Among the various renewable fuels, hydrogen is playing an increasingly important role and represents a key junction between the sustainability concept pursued and the very functionality of future decarbonized energy systems. Hydrogen used in combination with other technologies has the potential to contribute to increasingly sustainable and clean industrial processes, zero-emission mobility systems and reduced emissions from domestic heating. In Italy, for example, such a scenario would lead to a reduction in CO_2 emissions of over 97 million tonnes, or 28% of total emissions. In addition, hydrogen has the capacity to connect the gas and electricity sectors and thus to provide flexibility in the energy system, encouraging the increasing use of renewables [2].

Literature Review In the literature, one can find many scientific articles, produced in recent years, dealing with the topic of hydrogen production from biogas. In the following chapter, the main papers analyzed for this work will be presented, with a summary and the main results. These papers were very useful for the development of the methodology with which the main work of this thesis was carried out, which will be explained in the next chapter.

With regard to the anaerobic digestion process, the study [3] shows how the concentration of hydrogen in anaerobic systems can be improved through processes such as the inhibition of micro-organisms, with the function of lowering the hydrogen concentration and promoting constant hydrogen removal in order to promote hydrogen-producing bacteria. Research in this field shows that such a process is

feasible, with limitations from an economic point of view, but at the same time promising results in terms of hydrogen yield. Efforts in this field show how hydrogen production is becoming increasingly important, with a focus on the transport sector where vehicles fuelled by tanks containing pressurised hydrogen in addition to an on-board battery can provide an alternative to current high-polluting systems. The article offers an overview of membrane reactors and solutions for separating methane from hydrogen using proton exchange membranes (PEM), which, using little energy, succeed in separating methane and hydrogen almost completely.

The article shows how, according to EPA estimates, the costs for a conventional in-house anaerobic digester range from 400,000 to 5,000,000 dollars with an average of $1.2 million. In the process of co-production of hydrogen and biogas, therefore, it can be seen that a one-stage or two-stage digester increases biogas production by 35 per cent and that the pre-treatment of the raw material and the microbial seed isolates the hydrogen and prevents its conversion into methane. Through this treatment, methanogenic bacteria do not convert hydrogen into methane, thereby increasing the partial pressure of hydrogen and the concentration of volatile fatty acids. Of particular importance is the evidence that a two-stage reactor fed with food waste through continuous hydrogen extraction and pre-treatment techniques can have the highest hydrogen production, compared to conventional processes. The production of biohydrogen also finds much space nowadays, precisely because of the importance attached to limiting CO_2 emissions in the sector. The article [4] presents simulation models for biohydrogen from agricultural waste, which, based on probability theory and mathematical statistics, show how such projects will become more profitable from 2030 onwards. In particular, it shows how some European countries, such as Sweden and Norway, have focused on the use of hydrogen in the transport sector and how Germany is using its existing gas infrastructure to mix natural gas with 'hydrogen and create fueling stations for cars. Studies show that the production risk for projects to develop biohydrogen from agricultural feedstocks, which is still high today, will become lower and lower from 2030 onwards and thus valuable to investors. The trend will be towards an increase in such projects. Based on the research, it is established that the expected increase in biohydrogen production projects, and related technologies, will reduce the total production costs.

As far as trends in project profitability change are concerned, one has:

- in 2030, at the minimum yield demand of $0.1-0.2/kg, the risk of obtaining biohydrogen from agricultural feedstocks will be 'acceptable', at $0.3-0.5/kg-'medium', at $0.6-0.8/kg-'high', and above $0.9/kg-'critical';

- in 2050, these indicators will improve significantly. Together with the changes in the minimum return on investment in biohydrogen production to 0.1-1.0 $/kilogram, the expected profit risk will change from "minimal" to "medium".

SMR hydrogen production represents a widely used and mature technology, in the literature there are many recent studies referring to this process such as [5] where the study concerning the production of hydrogen from biogas in an industrial-scale reformer is presented. A one-dimensional non-isothermal reactor model was formed using mass, momentum and energy balances. The model equations were solved using MATLAB software. The developed model was validated against available modelling studies on industrial steam reforming of methane and those on laboratory-scale steam reforming of biogas. The effect of changing biogas composition on industrial steam reformer performance was studied in terms of methane conversion, hydrogen and carbon monoxide yields, product gas compositions, reactor temperature and total pressure. The biogas compositions $CH_4/CO_2 = 40/60$ to $80/20$), S/C ratio, reformer feed temperature and heat flow were varied. The preferred feed conditions for the reformer are a molar feed of 21 kmol/h, steam-to-methane ratio of 4.0, temperature of 973 K and pressure of 25 bar. Under these conditions, the biogas-fuelled industrial reformer provides methane conversion (93.08 and 85.65 %) and hydrogen yield (1.02 and 2.28), which are close to thermodynamic equilibrium conditions. The endothermic process of steam reforming (operated at high temperature, 973 and 1273K) and the various reactions involved are then presented, drawing on other scientific studies. The industrial reformer is then presented, consisting of 40 to 400 tubes, 70 to 10 mm in diameter and 6 to 12 m long m catalysed with Ni. Simulations were carried out to evaluate the performance of an industrial-scale steam reformer for SRB with varying biogas composition $CH_4/CO_2 = 40/60, 50/50, 60/40, 70/30$ and $80/20$ with the heat flow varying between 0 and 70 kW/m^2.

A heat flow of 65 kW/m^2 was found to be suitable for the biogas feeding conditions, i.e. total feed rate = 21 km/h, $S/C = 4.0$, T=973 K and P=25 bar. Under these conditions, the industrial-scale reformer fed with biogas of different compositions reaches values close to thermodynamic equilibrium. It gives the methane conversion (93.08 and 85.65 %), steam conversion (17.37 and 28.34%), carbon monoxide yield (0.467 and 0.463 mol/mol BG)), and the molar percentage of hydrogen on a dry basis in the outlet gas (50.56 and 69.49%) for the biogas composition $CH_4/CO_2 = 40/60$ and $80/20$. Furthermore, the temperature of the outlet gas varies between 1142 and 1115 K, and the total pressure at the reactor outlet is in the range of 22.36 and 22.91 bar.

As will be explained later in the chapter 3 the feedstocks from which to produce biogas in the AD process are different, each of which has different yields. In the article proposed by [6], the use of organic waste in agribusiness is analyzed, in particular, those generated from livestock and crops that represent an opportunity for biofuel production from biogas plants. In the article, the complete hydrogen production cycle is analyzed, starting from the collection and preparation of the feedstock, ultrasonic treatment, anaerobic digestion, biogas storage, biogas purifi-

cation, steam reforming of methane at 1073 K , and purification of the obtained hydrogen. The article notes that it is easier to co-digest animal and plant waste in centralised biogas plants. Co-digestion improves the course of methanogenesis and increases the biogas yield. Two-stage anaerobic fermentation allowed biogas and biohydrogen to be formed. It has been observed that this technology for utilising liquid organic waste is energy-efficient; to obtain 1 $m^3$of hydrogen, 1.1 kW h of electricity is required. It is pointed out how steam reforming of biogas is one of the most convenient and promising methods of producing hydrogen. Various scenarios for biogas formation from livestock farms are then analysed. For the numerical implementation of the mathematical model and the heat and mass transfer processes during methane steam reforming, the software package COMSOL Multiphysics 3.5 is used, which allows systems of non-linear partial differential equations to be solved using the finite element method.

In the study carried out by [7] the potential of hydrogen from biogas by steam reforming and WGS processes is analyzed, starting from pig manure, which is considered a pollutant if not properly treated. The results obtained show that the ecological efficiency, pollution indicator and energy efficiency of the process measure 97.73%, 19.15% and 76.06%, respectively, demonstrating the feasibility from the ecological point of view; the payback of the 8-year plant with H_2 production at a cost of \$0.14/ kW h in a production scenario of 8760 h/year, showing an exergetic efficiency of 76%.

The data required to perform the study were acquired from a predictive simulation model implemented in Aspen Hysys by setting the thermodynamic problem with the method PSRK (Predictive Soave Redlich Kwong). Compared to other studies dealing with the technical analysis of hydrogen production using SRM and WGS, the main novelty of this study lies in the simulation and subsequent exergetic analysis of hydrogen production. In the section on energy efficiency, it was observed that most of the irreversibility of the production process occurs in the reformer (41.37%) and steam generator (24.75%), thus, these are equipment that could have technological improvements to improve process efficiency. Still remaining in the scenario of hydrogen production by SMR, many studies analyze the behavior of the process when using membrane reactors; [8] propose a study in which the conventional SMR process using nickel catalysts is compared with a process in which a PdAu membrane reactor is used for small-scale production. The model is simulated with Aspen Plus software, using a pressure of 30 bar and a temperature of 550 °C for the reformer, while for the conventional process the pressure and temperature of the reformer are 23 bar and 900 °C. The study shows that the process using the membrane reactor has higher values for methane conversion, hydrogen yield and efficiency. The results show that when the reforming reactor in conventional SMR is operated at temperatures below 900 °C, the energy efficiency decreases due to low methane con-

version. The economic analysis (bottom up) shows that the cost of hydrogen for the conventional SMR process is \$4.54/ kg while for the process using the membrane reactor \$2.88/ kg. Continuing the analysis of membrane reactors there are studies conducted on non-commercial reactors such as the one proposed by [9]. The study proposes the steam reforming of a synthetic biogas stream containing 200 ppm H_2S , carried out in a non-commercial membrane-supported $PdAu/Al_2O_3$ reactor (7 and 8 mm selective layer thickness)at 823 K and 150 kPa on a $Rh(1\%)/MgAl_2O_4/Al_2O_3$. This system is capable of recovering almost 80% of the total hydrogen produced during the reaction and shows good resistance to H_2S contamination, as confirmed by stable methane conversions for more than 400 hours of operation. For comparison, the same reaction was carried out in a commercial self-supporting PdAg membrane (150 mm wall thickness), achieving 40% hydrogen recovery at 623K and 200 kPa, and exhibiting stable methane conversions for less than 200 hours of operation due to the effect of H_2S contamination.

After the technological description of the membrane, the tests performed are described, in particular, pure H_2 permeation tests were conducted between 573 and 823 K, varying the transmembrane pressure between 0 and 100 kPa. The flux of H_2 permeating through the membrane increased by increasing the transmembrane pressure (the higher the transmembrane pressure, the higher the driving force of H_2 permeation) and temperature. In particular, an increase in temperature allowed for an increase in H_2 permeation flux; in fact, H_2 permeability depends on temperature according to an Arrhenius-type equation.

The apparent activation energy (EA) was graphically estimated at 50 kPa transmembrane pressure from the graph of which gives 12.1 kJ/mol with the correlation coefficient $R_2 \sim 0.97$, thus comparable to other literature data . In the hydrogen production scenario, the power-to-gas (PtG) concept is very important, with a focus on methods of hydrogen production by means of electrolysis enhanced by renewable sources. the study proposed by [10] presents this concept for the production of hydrogen for end uses such as transport, natural gas distribution network. The study focuses on methods for producing hydrogen from the electrolysis of water using SOEC, SOE, PEM, Alkaline, and highlights the relevant operating parameters. It is shown how, due to the lower density of hydrogen, the volume-dependent heating values of hydrogen are lower than those of methane, while the mass-dependent heating values are higher. The study also lists several PtG-related projects being implemented in Europe.

Plant CF, CAPEX and OPEX, hydrogen cost and efficiency for fuel cells powered by different renewable energy sources are also analysed. In particular, it can be seen that a PEM powered by PV has a higher electricity cost, zero hydrogen cost, but lower efficiency than all others. In this review, some conclusions are summarised as follows:

- The PtH concept, which produces hydrogen with the PEM electrolyser, has fewer environmental consequences than other conventional processes such as coal gasification and steam methane reforming. The environmental impacts of this technology may change depending on the source of the electricity supplied to the PEM electrolyser. For example, the use of coal may increase impacts on freshwater eutrophication, and the use of nuclear energy may increase impacts of ionizing radiation

- Energy sources are economically studied for PtH systems. The geothermal-based system has the highest normalised levelised cost of electricity of 6.21 during hydrogen production, while natural gas has the lowest normalised value of 0. On the other hand, the highest CAPEX and normalised fixed costs belong to the natural gas option as 7.42 and 8.82, respectively.

- Electrolysis technologies powered by different energy sources are also compared with each other in terms of efficiency, capacity and cost. The best case for plant efficiency is valid for high-temperature electrolysis fed by biogas with a normalised value of 9.40. In comparison, the lowest normalised efficiency appears to be 0.98, which belongs to the solar PV driven PEM electrolyser. The highest normalised cost is found at 7.96, which is valid for high-temperature steam electrolysis driven by electricity from biogas. In comparison, the lowest normalised cost is 0, which belongs to the solar PV-powered PEM electrolyser.

The aim of this work is to investigate the production process of H_2 through steam reforming of biogas, assessing its economic feasibility, comparing this process with the production of hydrogen through electrolysis with the use of fuel cells powered by electricity obtained from the use of photovoltaic panels or other renewable sources.

For this purpose, thanks to the Aspen Plus software, a hydrogen production power plant powered by a biogas flow of 59.05 kg/h was simulated. The biogas flow is derived from an AD plant of the WWTP type, the reforming reactor used is not a membrane reactor and will be studied with an analysis referring to reforming temperatures decreasing from 900°C to 700 °C .Of the various processes analysed, a pinch analysis will then be carried out, calculating in particular the heat that can be recovered from the process, and the minimum heat required for the process, this being a key figure in the calculation of process efficiency. Remaining in the context of pinch analysis, for each process analysed, a network of heat exchangers is proposed; this optimisation was conducted using the Aspen Energy Analyzer V10 software. For the base case, i.e. BSR with a reforming temperature of 900 °C, the economic analysis with LCOH calculation is proposed.

Structure Following this introduction in which the importance of hydrogen in the world energy scenario was analysed, and a review of the recent literature in the field

of biogas and hydrogen, the second chapter summarises the hydrogen production methods, describing the steam reforming process and the electrolysis process in detail. The third chapter describes the production of biogas, which can be derived from various raw materials, from the anaerobic digestion process. Biogas upgrading technologies are then described. In the fourth chapter, an analysis of the global, European and Italian biogas potential is made. In the fifth chapter, the methodology behind the work is illustrated, so the input data for the model developed with the Aspen Plus software is described; the pinch analysis procedure and the choice of the number of exchangers are described; the economic analysis and the input data required to arrive at the LCOH calculation are explained. Finally, in the sixth chapter, the results obtained for the various parts of the study performed are proposed.

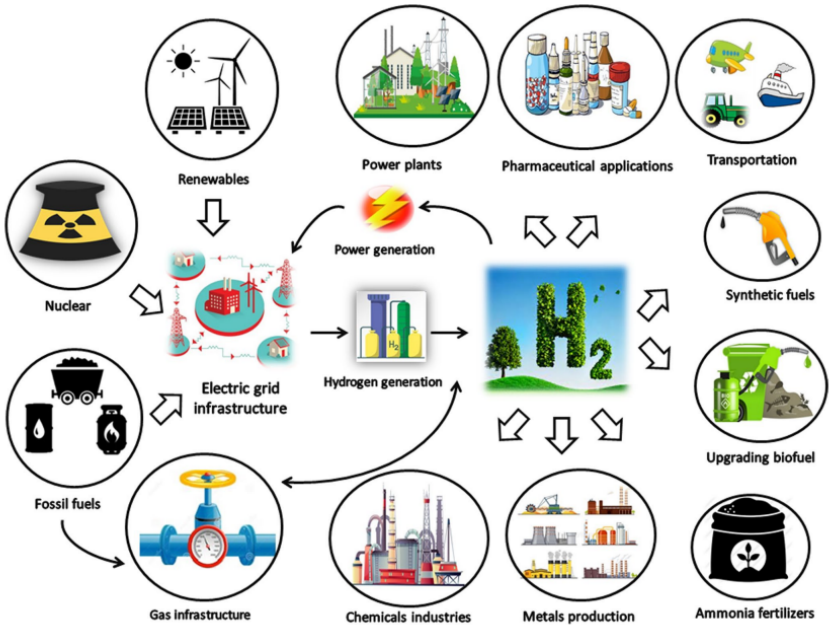

Figure 1.1: Hydrogen production routes, including renewables, fossil fuels and nuclear, with hydrogen being produced in power plants, pharmaceutical applications, synthetic fuels or their upgrades in transportation, ammonia synthesis, metal production or chemical industry applications [11]

Chapter 2

Hydrogen production methods

Hydrogen in pure form does not occur in nature, however, it can be produced by various chemical and physical processes. Depending on production methods, raw materials and resources used, GHG emissions, different types of hydrogen can be distinguished. In particular conventional, *low-*CO_2, *free-*CO_2, carbon-free production is distinguished by reference to colors, such as "grey", "turquoise", "blue" ,"green", "brown" and "pink" [12].

- Grey hydrogen: H_2 produced by steam methene reforming;
- Blue hydrogen: H_2 produced by SMR combined with carbon capture and storage;
- Turquoise hydrogen: H_2 produced by methane pyrolysis;
- Green hydrogen: H_2 produced by polymer electrolyte membrane water electrolysis, or, produced tanks to the valorization of bioresources such as biogas.
- Brown hydrogen: H_2 produced by the gasification of coal-based fuel.
- Pink hydrogen: H_2 produced by electrolysis powered by nuclear

Based on these energy sources, various methods of hydrogen production can therefore be distinguished. Currently, the vast majority of hydrogen production is based on thermochemical processes using fossil fuels. 96% of the hydrogen produced worldwide is generated from fossil fuels (49% from natural gas, 29% from liquid hydrocarbons). To this percentage must be added 4% hydrogen produced by electrolysis and other hydrogen sources. Thermochemical processes from fossil fuels include hydrocarbon reforming, coal gasification, hydrocarbon pyrolysis and plasma reforming [14]. The state of the art of the steam methane reforming and of the electrolysis is briefly outlined below. First we can say that the reforming is

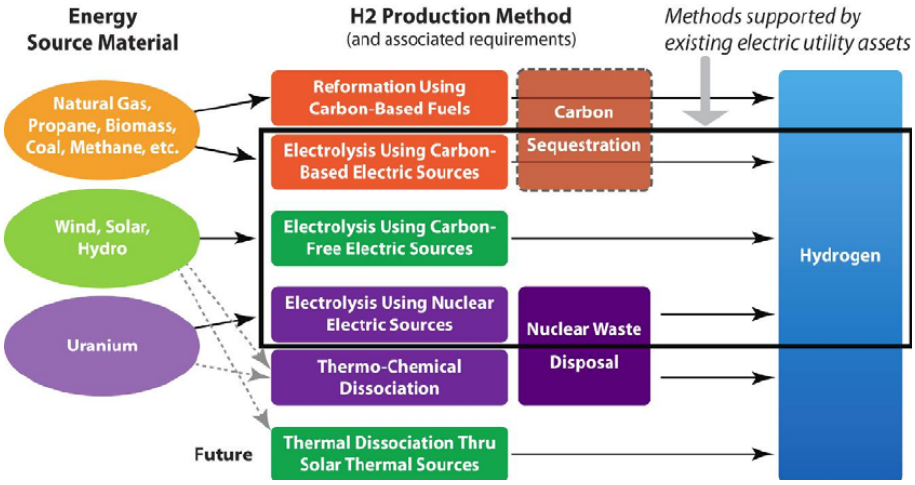

Figure 2.1: Hydrogen production pathway [13]

a process that, depending on the reactants, can be classified into steam reforming, partial oxidation and autothermal reforming. The steam reforming is an endothermic catalytic process leading to the generation of hydrogen-rich syngas. When the process is fuelled by natural gas, it is referred to as SMR.

Steam methane reforming: This represents the most widely used technology to date for producing hydrogen. As a fossil fuel-based production method, the resulting CO_2 emissions are not negligible and contribute to climate change, albeit with a less significant impact than the direct use of fossil fuels for energy production. As far as the process is concerned, overall it is divided into three steps: reforming or syngas generation, WGS, a reaction to increase the hydrogen content of the syngas (H_2/CO) ratio and finally gas purification with CO_2 separation. Thanks to a catalytic tube reactor, natural gas is endothermically converted into syngas. The endothermic reaction of the SMR is favoured at high temperatures and H_2/CO ratio has values around 3 or higher. Important in the process is to maintain a sufficiently high reforming temperature in order to avoid catalyst cracking, which can be achieved by burning natural gas. If the natural gas has organic sulphur components in its composition, a desulphurisation unit must be added upstream of the reformer catalyst. The next step is WGS, preceded by a heat recovery system into which the gas mixture enters, thanks to this step the steam is converted to CO_2 and H_2. The gas mixture then enters a unit for CO_2 removal and a methanation process, or through a pressure adsorption process to obtain pure hydrogen. For the steam reforming process, one of the most important factors is the ratio of hydrogen to carbon in the raw material, in fact, the lower this factor, the greater the CO_2 emissions. To achieve a higher overall reaction rate, a membrane reactor can be used,

thus replacing reforming and WGS. Currently, studies are focusing on processes that can replace the use of conventional reformers, such as membrane reactors and fluidised bed reactors. The catalyst is also an element of ongoing research, precisely because of the increase in hydrogen yield achieved by reducing the negative effect of sulphur and carbon deposition [14].

Electrolysis: Electrolysis is the innovative process for the carbon-free production of hydrogen by harnessing energy from renewable and nuclear sources. The process involves using electricity to split water molecules into hydrogen and oxygen. This reaction takes place in units called electrolyser, which, similar to fuel cells, consist of two parts, an anode and a cathode separated by an electrolyte. Depending on the electrolyte used, i.e. its material, conduction of different types of ions can occur [15]. Through electrical power, therefore, water is split, the resulting hydrogen is sent to the cathode, and oxygen to the anode. The electrolyser placed between the two electrodes has the characteristic of being an ion conductor and an electrical insulator. Electrolysers are of the polymer electrolite membrane, acidic (PEM), alkalini and solid oxide electrolyte types. The ions exchanged via the electrolyte are H+, OH- or O. PEMs are capable of working at low temperatures (<80 °C), AELs at moderate temperatures (<220 °C); PEMs have a low hydrogen production capacity (< 30 Nm3/H) and not very high efficiencies, whereas akalines show higher efficiencies and production capacities. The discussion changes when using solid oxide electrolysers, which have different characteristics and can be processed at high temperatures (>600 °C) [16], resulting in greater adaptability for large-scale hydrogen production methods.

Chapter 3

Biogas production from anaerobic digestion

Biogas is a mixture of methane, CO_2 and other gases present in small quantities that results from the process of anaerobic digestion of organic matter in an oxygen-free environment [17]. The composition of biogas also varies depending on the raw materials from which it is produced. In fact, biogas can have different origins depending on whether it is produced from plant biomass, substances of animal origin or waste. Biogas is odourless, while the solid and liquid fraction, known as "digestate", produced from the anaerobic digestion process has an important agronomic value. In addition biogas is 100% renewable (no new carbon); transportable and storable; permanently available; upcycles low-grade organic waste into a high-value energy source. The large energy potential of biogas translates into the possibility of producing electricity using this resource in thermal power plants, or for the production of heating and hot water for end uses, also using a district heating network. Heat and electricity can also be integrated into a single cogeneration system, maximizing the energy efficiency of the system. Among other uses of biogas, specifically biomethane, is in the automotive sector, where a pathway is being explored that would lead to a replacement of fossil-origin methane gas. As mentioned above, a wide variety of feedstocks can be used to produce biogas such as animal manure, crop residues, organic fraction of municipal solid waste, including also industrial waste and wastewater sludges [17].

Crops residues: following the harvesting of certain crops such as wheat, maize, sugar cane and rice, a large quantity of residues such as husks, wheat straw, rice straw are produced, which can be used as a biomass energy resource [18].

Animal manure: animal manure is an excellent substrate for anaerobic digestion with a carbon-nitrogen ratio of 25:1 and rich in nutrients necessary for the growth

Composition	Natural Gas	Biogas			
		Waste Water	Food Waste	Animal Waste	Landfill
Methane [% vol.]	80-100	50-60	50-70	45-60	40-55
Carbon dioxide [% vol.]	<3	30-40	25-45	35-50	35-50
Nitrogen [% vol.]	<3	<4	<4	<4	<20
Oxygen [% vol.]	<0.2	<1	<1	<1	<2
H_2S[ppm]	<0.1	<400	<10000	<300	<200
Non H_2S sulfur [ppm]	<10	<1	<1000	<30	<30
Halogens [ppm]	<0.1	<0.2	<0.2	<0.2	<100
Moisture [%]	<0.02	~ 3	~ 3	~ 3	~ 3

Table 3.1: Biogas composition of different origins

of anaerobic microorganisms, so it is an accessible and cheap resource [19].

Wastewater sludge: fraction of solid matter contained in municipal and suburban wastewater that is removed by sewage treatment plants in the form of gas.

Organic fraction of municipal solid waste: OFMSW is considered as green and food waste, paper, cardboard, wood and also waste from parks, gardens and kitchens. these can also be used in landfills to produce landfill gas [17] [20].

The anaerobic digestion process allows the above-mentioned feedstocks to be transformed into biogas or digestate. The process of anaerobic digestion represents a complicated four-stage degradation process:

- Hydrolysis;
- Acidogenesis;
- Acetogenesis;
- Methanogenesis.

Hydrolysis: is the process in which complex organic substances such as proteins, carbohydrates and fats are converted into smaller molecules such as amino acids, sugars and fatty acids. This action is carried out by extracellular enzymes that enable, and facilitate, transport within the microbial cell [21].

Acidogenesis: also known as fermentation, is the process by which molecules from the hydrolysis process are converted by acidogenic microorganisms into short-chain fatty acids (known as VFA), CO_2, H_2 *gas*, alcohols, nitrogen compounds, organic acids and some organic sulfur compounds [21], [22].

Acetogenesis: is the third stage of AD where there is complete acid formation through the fermentation of carbohydrates leading to the production of acetate, CO_2 and hydrogen, components that can be used in the next stage to produce methane by methanogens [23].

Methanogenesis: is final stage of anaerobic digestion. In this stage, all the products resulting from acetogenesis and some intermediate products resulting from hydrolysis and acidogenesis through methanogenic agents create methane. Methane is produced through three pathways: aceticlastic, hydrogenotrophic, methyltrophic methanogenesis. Most methane is produced from the products of acetogenesis (acetate) in CH_4 and CO_2 thanks to the following reaction:

$$CH_3COOH \rightarrow CH_4 + CO_2 \tag{3.1}$$

then thanks to reactions 3.2 and 3.3 the hydrogenotrophic group converts H_2 and CO_2 into methane and H_2O , from this pathway approximately 30 % CH_4 is produced [21], [23].

$$CO_2 + 4H_2 \rightarrow CH_4 + 2H_2O \tag{3.2}$$

$$4CO + 2H_2O \rightarrow CH_4 + 3CO_2 \tag{3.3}$$

Of considerable importance in the AD process is the need to maintain a balance between the population of methanogenic microorganisms and hydrolytic, acidogenic and acetogenic microorganisms, which are heterotrophic, i.e. consume complex organic substances. The methanogens reproduce at a slower rate than the components of the first three stages of AD, which is why it is important to ensure an adequate population of these bacteria, in fact, if these are insufficient, the VFA are accumulated, acting to the detriment of the methanogens, for which they are toxic. By controlling the rate at which the waste remains in the digester (residence or retention rate), the desired result can be achieved, which is to maintain a higher growth rate of methanogens than the rate of loss in the reactor effluent. AD systems, in most cases, consist of a single reactor in which acetic acid, hydrogen, carbon dioxide

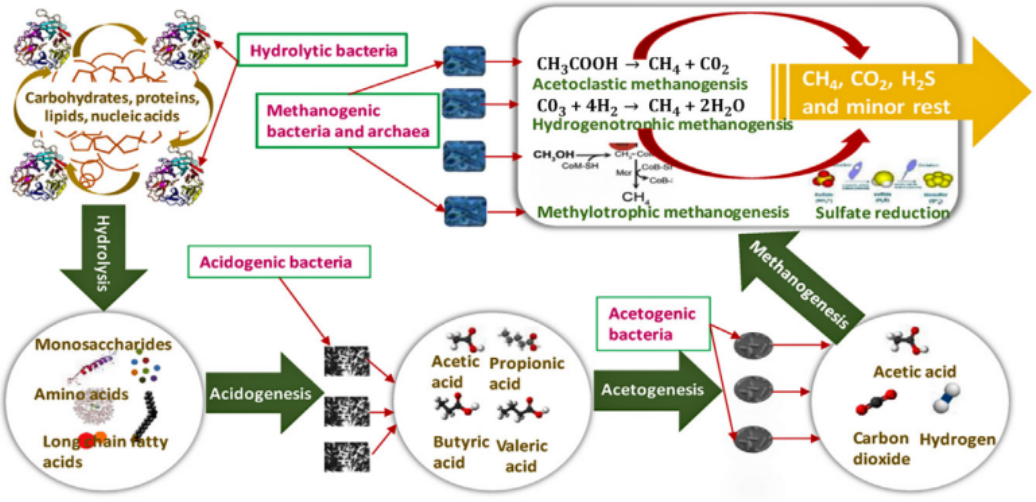

Figure 3.1: Anerobic Digestion process [21]

and methane are produced currently. Theoretically, processes in which there is a separation of the microorganisms should allow for greater, and thus more precise, control of the process. In this case, the digesters are divided into two stages; a first reactor in which there are microorganisms from the first three steps of AD (hydrolysis, acidogenesis, acetogenesis), and a downstream reactor in which there are microorganisms that form methane. This phase separation, however, has not shown significant advantages over single-phase AD, which is precisely why the best engineering choice to be made for the construction of a digester depends on the type of raw material used and converted in the digester, given the wide range of process options; it also depends on a variety of design, operational and cost reasons. There is, therefore, no single AD/biogas system or technology that works best for all feedstocks [24].

3.1 Biogas upgrading technologies

Following the production of biogas from the anaerobic digestion process, a further step is the biogas upgrading process, which is an internationally interesting technology. It is precisely this process by which methane is produced from a renewable fuel such as biogas that represents a method for generating an alternative to fossil methane. As specified above, the biogas obtained from the anaerobic digestion process contains more than 50 % methane, an also significant proportion of CO_2 and minimal parts of other substances including hydrogen sulphide H_2S and steam. The

biogas obtained from AD consists of a high percentage of methane, and represents a great potential for limiting the use of fossil fuels, however, it cannot be used as a widespread energy carrier. In addition, the presence of CO_2 does not allow methane to be used in the public network or to be used as an automotive fuel. In view of these reasons, technological progress in methods of extracting CO_2 from biogas resulting from AD has become an increasingly important issue. Biogas upgrading is precisely the process by which CO_2 is separated from biogas, allowing the production of biomethane, an energy carrier with characteristics similar to those of natural gas, and from renewable sources [25].

There are multiple technologies for biogas upgrading. All have advantages and disadvantages and different ones can be suitable to different project cases depending on local particulars. The most popular ones include:

- **Permeation** : technology that uses special membranes for purification to take place it is generally a multi-stage process. The process can be characterised by high-pressure gas separation with gas phases on both sides of the membrane, or, low-pressure liquid absorption, in which case a liquid absorbs the molecules diffusing through the membrane.

- **Pressure swing adsorption (PSA)** : gas separation takes place under pressure, in particular, at temperatures close to ambient, gases are adsorbed based on molecular characteristics and affinity to an adsorbent material. As far as materials are concerned, activated carbon, silica gel and activated alumina adsorb CO_2; molecular sieves adsorb carbon monoxide.

- **Water scrubbing** : thanks to this technology, it is possible to remove CO_2 and hydrogen sulphide as they are more soluble in water than methane. it is a physical process in which the adsorption process takes place counter-currently. The biogas is fed under pressure into a packed column in the lower part, while water is fed into the upper part.

- **Physical absorption** : process in which an organic solvent absorbs CO_2. A typical solvent for this purpose is the polyethylene glycol.

- **Chemical absorption** : technology using different adsorbing agents such as organic amines. In this case, the CO_2 binds chemically to the liquid and also reacts with the amine.

- **Cryogenic upgrading** : less common process than the others due to the high energy intensity required, as it consists of an initial compression of the biogas, followed by cooling and finally an expansion. Through this process, the CO_2 is condensed and in turn also the methane, but at a lower temperature. The other

gas components are then selectively distilled at their boiling temperatures. The result is gases of high purity [26].

Chapter 4

Biogas Potential Analysis

When talking about the future of biogas, in the global energy context, one cannot avoid also talking about biomethane (obtained through a biogas upgrading process). Thanks to the ongoing energy transition process, biogas and biomethane have a great opportunity to gain an established position in global energy consumption, in fact, these gases can lead to a significant decrease in the use of fossil fuels in parts of the energy system where low-carbon electricity cannot reach. As shown in the IEA's WEO on biogas and biomethane, where two scenarios such as the STEPS and SDS are analyzed, the market share of these combined fuels in bioenergy demand is growing from 5% to 12% by 2040 in the STEPS and 20% in the SDS. To date, Europe and North America are the regions with the highest production capacity, which stands at 60%. Europe, in particular, is the leading region for biogas production with approximately 20,000 plants, with Germany accounting for the majority. These plants supply electricity on site and are suitable for cogeneration, with around 500 plants for biogas upgrading. In STEPS, the projected biogas production in 2040 is around 75 Mtoe, thus more than doubling the 2018 figure (35 Mtoe). The main source in this sector is MSW from which energy is obtained for premises and heating. The share of biogas used for heat and energy also increased from 70% to 85% in 2040. This growth is also due to subsidies for the biogas market with incentives such as feed-in tariffs, tax breaks, and subsidies also for rural areas. Also important is the development of digesters in favorable areas such as places near power sources, electricity grids, local energy distribution; not only an opportunity is the development of technologies to treat wastewater. The last opportunity becomes very important in developing countries, which are expected to be a real engine for the growth of biogas production. In Asia today, there is a large production of biogas, and China plays an important role.

In the SDS scenario, however, political and economic support for biogas development results in a much higher increase in biogas production by 2040 than in STEPS [17] .

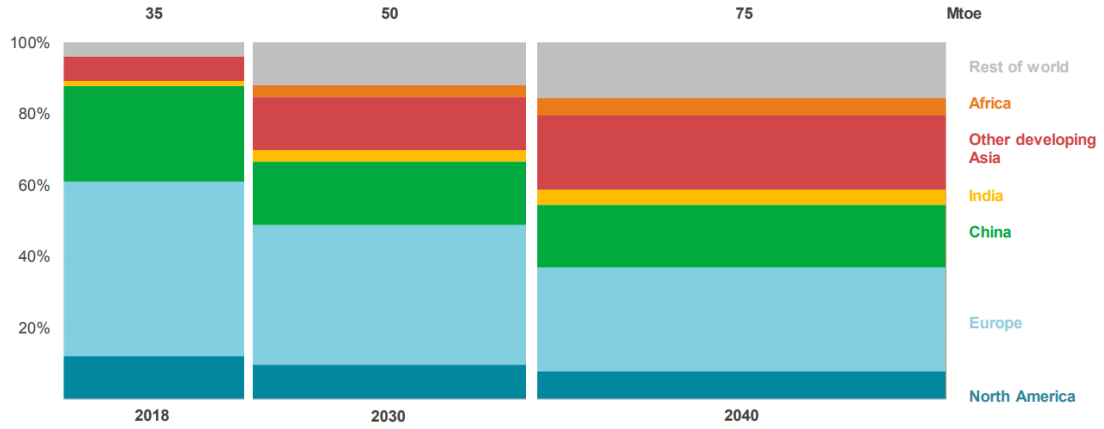

Figure 4.1: Global biogas demand for direct use in the STEPS [17]

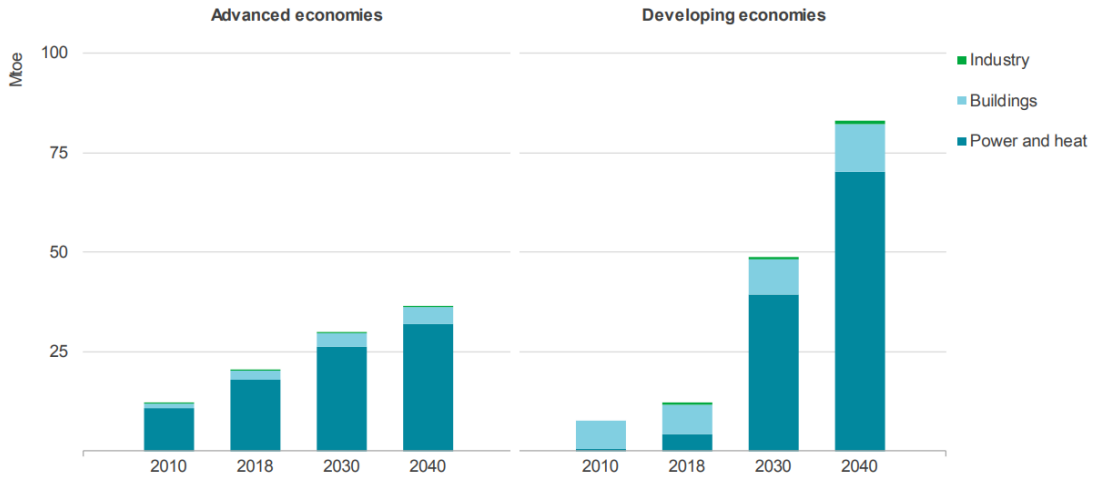

Figure 4.2: Global demand for direct use of biogas in the SDS [17]

As far as Europe is concerned, as mentioned earlier, Germany is the country with the largest biogas production capacity. Other countries developing new plants include France, Italy and Denmark. Italy, as shown in a study by the European Biogas Association, has increased its biomethane plants by 11 units by 2020, which places it among the countries with the greatest development of these technologies in Europe. Electricity produced, in Italy, from biogas is approximately 8,166 GWh, in 2020, the majority of which comes from northern Italian regions (83.4% of the total), in particular in the Po river valley, where cattle breeding and viticulture are widespread [27].

The thermal energy obtained from biogas in Italy in 2020 is approximately 13,000 TJ, while, direct consumption of biogas is 1,522 TJ, of which approximately 45% is

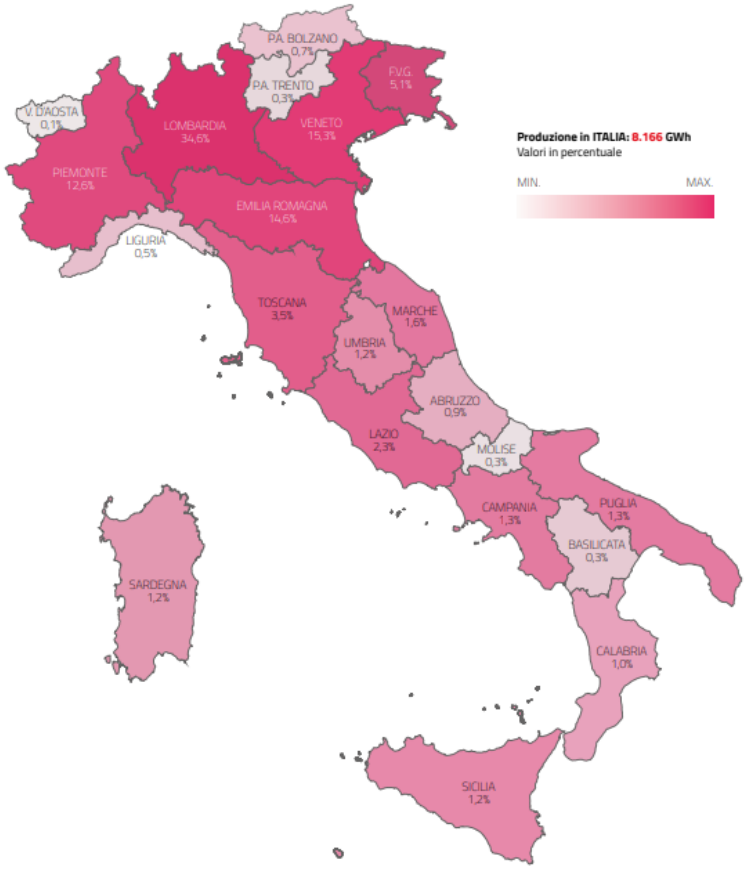

Figure 4.3: Regional distribution of electricity production from biogas plants in 2020 [28]

absorbed by the industrial sector and 55% by the trade and services sector; direct consumption in the residential sector has not been recorded. To this direct consumption must be added 11,474 TJ of heat from biogas-fuelled cogeneration plants and 3 TJ from heat-only plants.

Following the European RED II directives in which new criteria have been defined, for the sustainability of bioenergy, in Italy, plants for the production of biogas/biofuels that will come into operation on or after 1 January 2021 will have to respect a decrement of GHG emission of 65%.

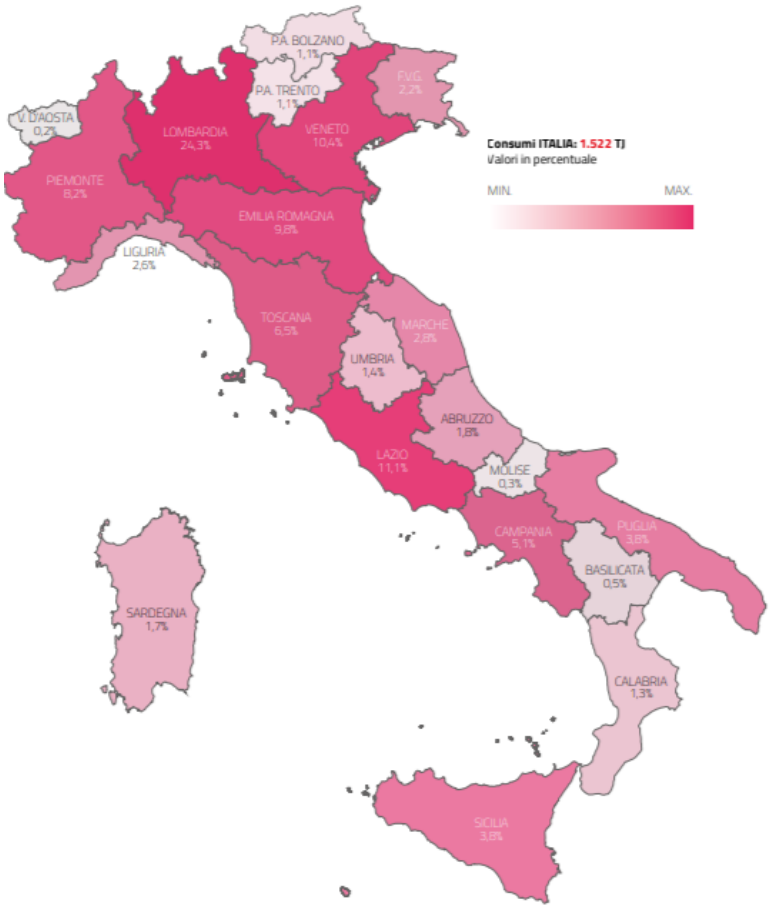

Figure 4.4: Regional distribution of direct biogas and biomethane consumption in 2020 (%) [28]

Chapter 5

Methodology

The model carried out using the Aspen Plus software is presented below, in which a hydrogen production plant was developed from biogas derived from an existing anaerobic digestion process.

The AD plant taken as a reference is the WWTP located in the city of Collegno (TO) in Piedmont, Italy, from which it was possible to obtain biogas production data for the year 2019. From this data, the average flow rate was extrapolated, which is then used as input in the model developed in the Aspen Plus software.

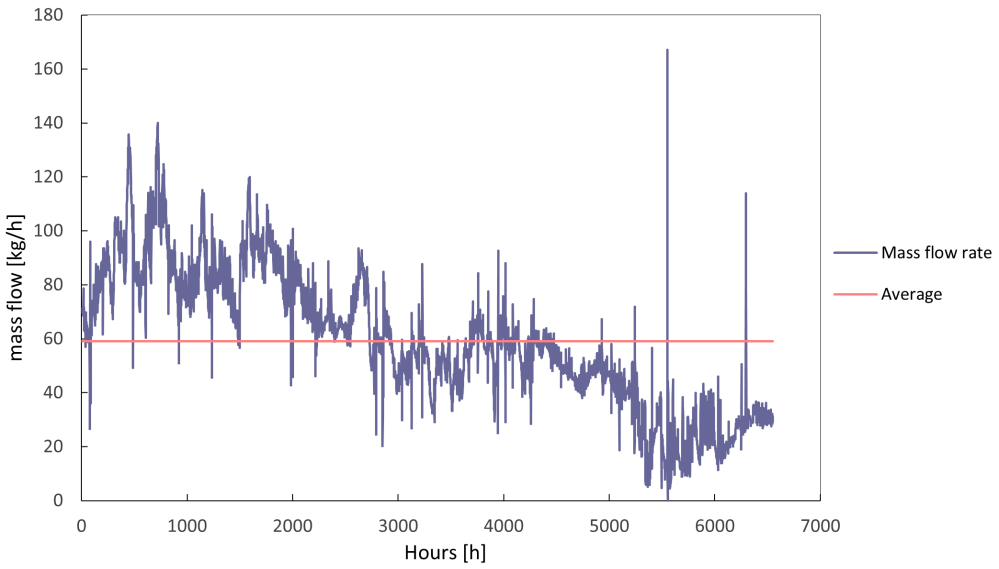

Figure 5.1: Mass flow rate of biogas produced in the year 2019 in the WWTP of Collegno

5.1 Aspen model description

The structure of the power plant represents the technology currently used to produce hydrogen from biogas.

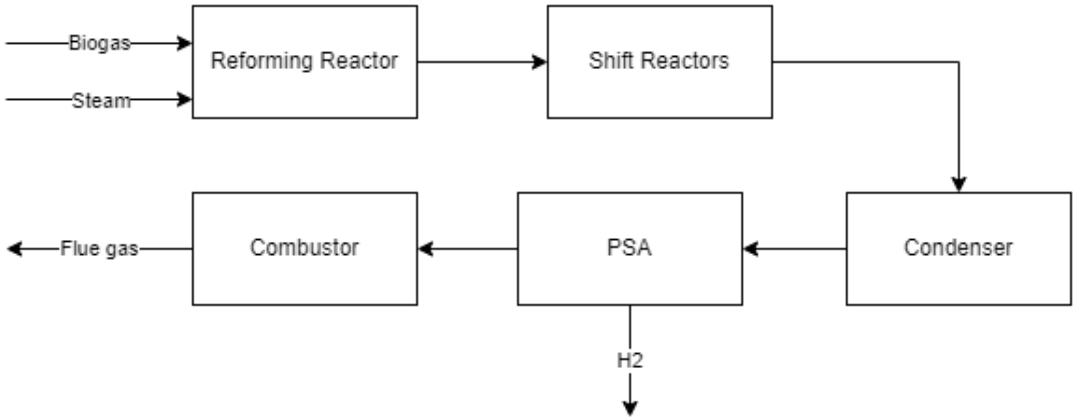

Figure 5.2: Biogas Steam Reforming process block diagram

As can be seen, the components entering the reformer are biogas and steam, the output product enters two WGS reactors, one at high temperature and the other at low temperature. Following the condenser, in which condensed water is extracted, there is the PSA unit, through which the hydrogen is separated with a purity of 99,99 %, the tail gases exiting the PSA undergo a high-temperature combustion process and the product, after being cooled, is sent to the atmosphere. In this study the French VABHYOGAZ3 project was taken as a reference for the construction of the model [29]. For the simulation, the Gibbs free energy minimization method was used, which allows the calculation of temperatures and composition at equilibrium under defined thermodynamic conditions. As the process is based on reforming, the components used as input in the Aspen Plus model are methane (CH_4), carbon dioxide (CO_2), carbon monoxide (CO), hydrogen (H_2), water (H_2O), solid carbon (C), oxygen (O_2) and nitrogen (N_2), representing air in a molar composition of $N_2/O_2 = 79/21$.

The basic method used in the simulations is PRMHV2 (Peng Robinson state equations modified with Huron-Vidal mixing rule), this method is an extension of Peng Robinson that can be used for both polar and non-polar components and can be chosen among the various method that we can find into the database of the software. On the basis of these initial assumptions, simulations were carried out at different reforming temperatures: 900 °C, 850°C, 800°C, 750°C, 700°C, all fed by the same biogas flow rate of 59.05 kg/h, which represents the average biogas production

Input data common for all the processes analysed	
Biogas molar composition (%)	
CH_4	59.7
CO_2	40.06
O_2	0.04
N_2	0.2
Biogas mass flow rate (kg/h)	59.09
Temperature HTWGS (°C)	350
Temperature LTWGS (°C)	210
Temperature PSA (°C)	38
Pressure Reformer (bar)	16
Pressure HTWGS (bar)	16
Pressure LTWGS (bar)	15.7
Pressure PSA (bar)	15.7
Pressure Combustor (bar)	1

Table 5.1: Common input data for plant layout in Aspen Plus

of the WWTP plant in Collegno (Figure 5.1). Biogas molar composition:

- $CH_4 = 59.7\%$
- $CO_2 = 40.06\%$
- $O_2 = 0.04\%$
- $N_2 = 0.2\%$

Other assumptions common to the various simulations are the temperature of the HWGS (350 °C), the temperature of the LTWGS (210 °C), the temperature of the PSA (38°C), the reformer, WGS and PSA pressure set at 16 bar, the pressure of combustion set to 1bar (see table 5.1).

The plant consists of a **compressor** with an isentropic efficiency set at 75% in which the incoming biogas is compressed, a **pump** in which the water entering the plant is compressed, the biogas is heated up to the reforming temperature by a **heater**, the same happens for the water obtaining steam.

The pump yeld is set at 75%.

Unit	Imposed conversion yield (%)
HTWGS	75
LTWGS	75
PSA	79

Table 5.2: Data common for all simulations, unit conversion yields

The biogas and the resulting steam are mixed by means of a **mixer** to obtain the stream that enters the **reforming reactor**. For this component, a Gibbs equilibrium reactor set at reforming temperature and 16 bar pressure was used in which the reaction

$$CH_4 + H_2O \rightarrow CO_2 + 3H_2 \tag{5.1}$$

takes place, and a methane conversion of 80% is imposed. The reformer at this temperature does not produce carbon. The stream leaving the reformer is then cooled by a cooler to the Water Gas Shift temperature of 350 °C that represent the HTWGS. For the **HTWGS**, a RStoic reactor was used by setting a CO conversion fraction of 75%, the reaction set:

$$CO_2 + H_2O \rightarrow CO_2 + H_2 \tag{5.2}$$

The resulting product is still cooled, because thanks to the exothermicity of the reaction the temperature increase, by means of a **cooler** to a temperature of 210 °C, that represent the temperature of the **LTWGS**. The same assumptions and component were adopted for this component as for HTWGS, in which the same reaction takes place. The product obtained is still cooled down to 38 °C so that it enters a **condenser**, for which a flash reactor was used, in which the water is separated, while the remaining mixture enters the **PSA unit**. For this unit, a separator was used in which a hydrogen split fraction of 79% was set. The pressure swing adsorption process enables pure hydrogen, pure at 99.99%, to be separated from the mixture. A flow of air is sent to the inlet of a **mixer**, mixing with the tail gas, product, obtained at the outlet of the PSA. A **heater** allows the temperature to be raised before entering the **combustor**, for which a RStoic reactor was used. This preheating is important to reach temperature for wich the combustion efficiency is maximized. The combustion products have high temperatures, so a **cooler** is inserted to lower the temperature to 200 °C so that the flue gases leave the atmosphere without inducing CO_2 condensing problems.

For the water required at the inlet to the plant, an automatic calculation was set up in the software's design specification, in which a steam to carbon ratio $S/C = 3$ was set and the calculation was done using Fortran. For the calculation of the air

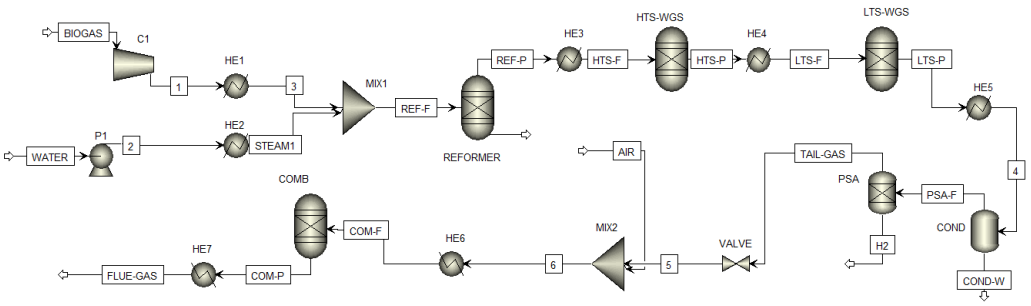

Figure 5.3: Biogas plant for the production of hydrogen

required at the inlet of the second mixer (MIX2), a calculator was used, setting the required stoichiometric air calculation in Fortran and adding an excess air of 10 %. The resulting air flow is calculated with the formula:

$$AF = (TG * \frac{2}{0.21} + TG1 * \frac{0.5}{0.21} + TG2 * \frac{0.5}{0.21}) * 1.1 \tag{5.3}$$

Where:

- TG = kmol/h of CH_4 contained into the TAIL GAS Stream
- $TG1$ = kmol/h of CO contained into the TAIL GAS Stream
- $TG2$ = kmol/h of H_2 contained into the TAIL GAS Stream

With this method, at each simulation these two inputs data are automatically updated according to the input data of the plant. From the data resulting from the simulations, it was possible to calculate for each simulation:

- the total energy required for heating and for the pump and compressor, E_{total} [kW];
- the thermal power calculated from the lower heating value, composition and mass flow rate of the biogas, $P_{LHV_{biogas}}$ [kW];
- the thermal power calculated from the lower calorific value, composition and mass flow rate of hydrogen $P_{LHV_{H_2}}$ [kW];
- the hydrogen production per process Q_{H_2} [kg/h];

- the energy consumed to produce 1 kg of hydrogen E_{H_2} [kWh/kg] computed with this formula:

$$E_{H_2} = \frac{E_{total}}{Q_{H_2}} \left[\frac{kW * h}{kg}\right] \tag{5.4}$$

And finally:

- the overall energy efficiency of the hydrogen production process, obtained as the ratio between the thermal power of the hydrogen produced and the sum of the thermal power of the biogas fed to the reformer and the hot service, and the electricity need

$$\eta = \frac{P_{LHV_{H_2}}}{(P_{LHV_{biogas}} + Q_{Hot_{min}} + Q_{el})} * 100 \tag{5.5}$$

5.2 Pinch Analysis

Pinch Analysis is a method for quantifying energy and energy-saving opportunities in the medium and long term for industrial processes, which often also translates into a reduction in plant costs [30] as this process can result in favorable optimizations not only from an energy but also an economic point of view.

Pinch Analysis is an engineering approach for calculating the reduction of energy consumption through the design of a heat exchanger network. Pinch analysis was carried out in this study using the Aspen Energy Analyzer V10 software, with which it was first possible to identify the composite curves. These are constructed by entering the inlet and outlet temperatures at the power plant units and their respective enthalpy values. A ΔT_{min} value is also set, which in this study was set at 15 °C.

Once the composite curves have been constructed, one referring to the cold utilities and one to the hot utilities, it can be seen how they approach at a certain point which represents the pinch point. This point is the closest point between the two curves where the temperature difference between the curves is precisely the set ΔT_{min}.

From the pinch analysis, it is also possible to quantify the remaining hot and cold tasks that are handled by the utility system. The hot utility Q_H represents the thermal energy to be supplied to the system from outside, the cold utility Q_c the thermal energy internally generated by the process but which can no longer be used by the process itself [29].

The first part of the simulation carried out in Aspen Energy Analyzer was based on the construction of composite curves and the evaluation of the thermal energy to be brought in from outside, the non-reusable thermal energy generated by the

system, and the recoverable thermal energy, with a graphical approach as shown in the figure 5.4.

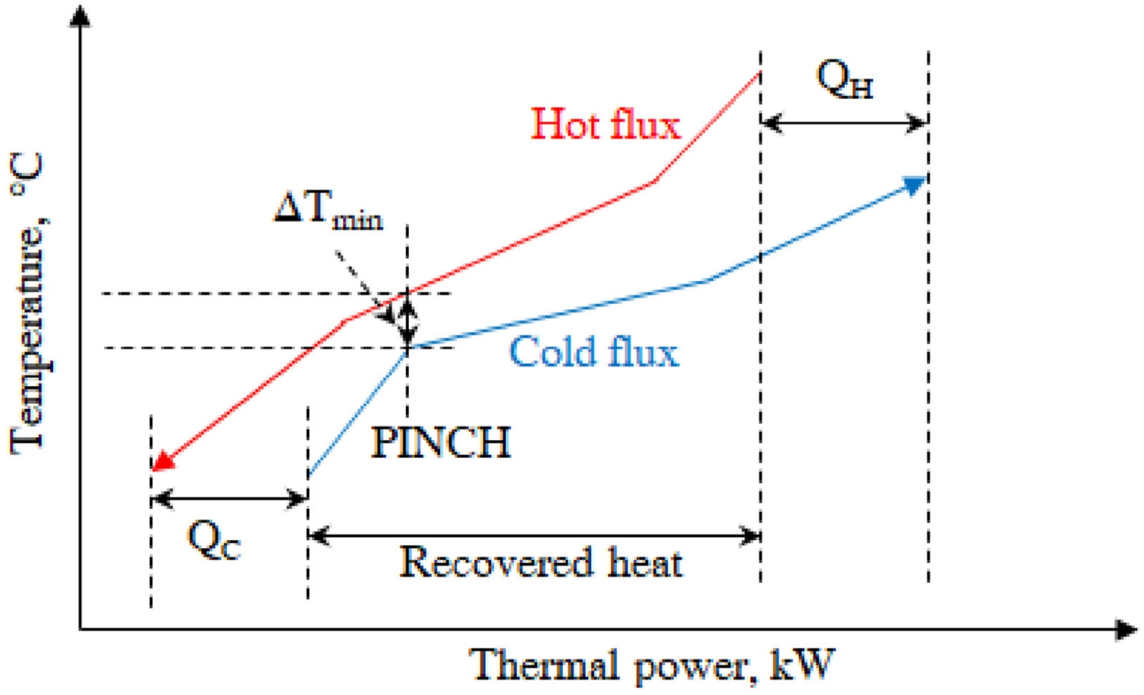

Figure 5.4: Pinch Analysis illustration of composite curves of a given process [29]

The next step of pinch analysis, again carried out with the Aspen Energy Analyzer V10 software, an optimization of the heat exchanger network for the simulated processes at different reforming temperatures is now proposed. The results were obtained by adding two utility streams to the model, one at low temperature, cooling water (<30 °C) and one at high temperature, very high temperature stream (1000 °C). The choice of the heat exchanger network is based on a discourse of minimising the insertion of the number of units, this at the expense of the efficiency of the system, but at the same time having a good compromise for what could be the investment cost of the intervention and in any case achieving a good yield of the system.

5.3 Economic Analysis

The economic analysis of the power plant is carried out with reference to the base case with a reforming temperature of 900 °C . In particular, the capital cost is calculated for each component of the power plant. The methodology used refers to that developed by the National Energy Technology Laboratory (NETL) [31].

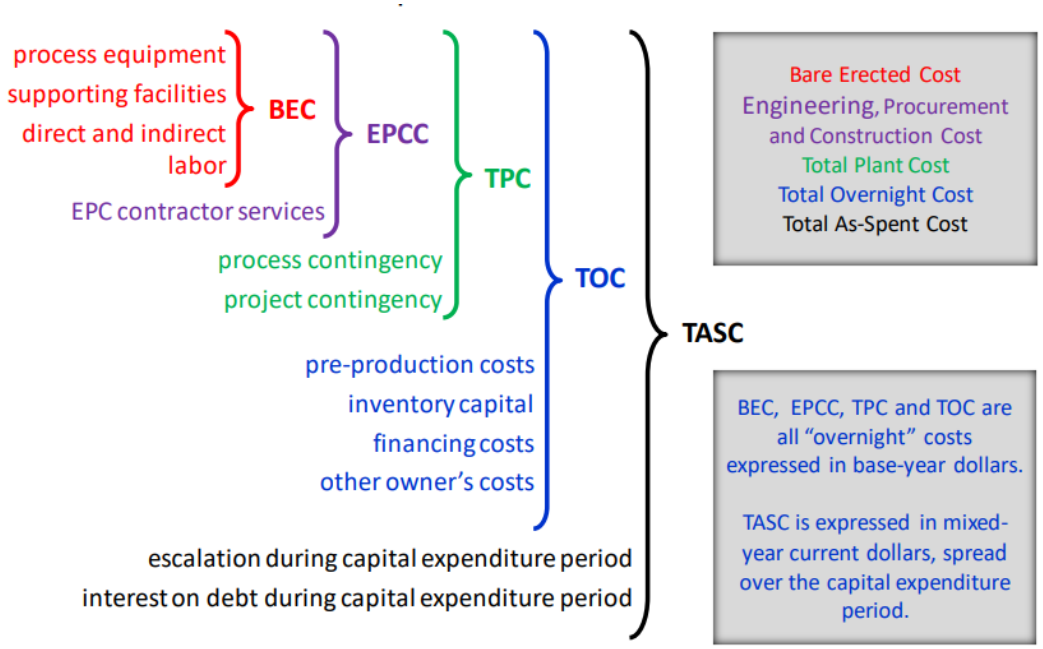

Figure 5.5: Capital cost levels and their elements [31]

There are five levels to be considered for capital cost calculation, as shown in Figure 5.5:

- The Bare Erected Cost (BEC) is comprised of the cost of process equipment, on-site facilities and infrastructure to support the plant including the labor to build/install them.

- The Engineering, Procurement and Construction Cost (EPCC) is inclusive of the BEC and the cost of EPC services. These services include detailed design, contractor permits (i.e., permits that contractors must obtain to perform the scopes of work, as opposed to project permits that are not included here), and project management and construction costs.

- The Total plant cost (TPC) includes EPCC plus project and process contingencies. This cost is a so-called overnight , expressed in base-year dollars and does not include escalation during construction or construction operating costs.

- Total overnight Capital (TOC): includes TPC plus all other "overnight" costs, including owner's costs. Since TOC is an overnight cost, it does not include escalation during construction and construction-related financing costs

- The Total as-spent capital (TASC) includes the sum of all capital expenditures incurred during the construction expenditure period, including their escalation. This cost also includes the interest that is incurred during construction in which there is the share on debt and from the return on equity (ROE). TASC is expressed in mixed, current-year dollars over the capital expenditure period.

BEC, EPCC, TPC, TOC are overnight costs expressed in base year dollars. The base year represents the year from which costs are calculated and the starting point for comparison between technologies. TASC, on the other hand, is expressed in mixed dollars of the current year for the full period of capital expenditure. The LCOH is, then, calculated by summing levelized capital costs in real terms to operation and maintenance (O&M) costs plus real fuel costs [31]. The LCOH is derived from:

$$LCOH = \frac{C_{inv} + \sum_{t=1}^{T} \frac{C_{FOM}}{(1+r)^t} + \sum_{t=1}^{T} \frac{C_{VOM}}{(1+r)^t}}{\sum_{t=1}^{T} \frac{M_{H_2}}{(1+r)^t}} \tag{5.6}$$

The equation 5.6 requires total investment cost and hydrogen production (M_{H_2}) to calculate hydrogen production cost in €/kg [35].

- The investment cost C_{inv} is represented by the total CAPEX;
- The term C_{FOM} refers to fixed operational and maintenance costs that are part of the OPEX;
- The term C_{VOM} refers to volatile operation and maintenance costs that are part of the OPEX;
- M_{H_2} refers the kg of hydrogen produced by the plant in one year of operation.
- E_{tot} refers to the total energy consumption to operate the plant multiplied by the total operating hours.

Those terms are discounted whit an interest rate of 3% (r) over the whole lifetime of the plant considered 25 years (t). The capacity factor of the plant is assumed to be 1. The cost of electricity and heat are referred to the ones of second half of the year 2020 in Italy, with reference to [32], [33], which are respectively 0.17 €/kW h and 0.3375 €/m^3 of natural gas.

The input data for the calculation of the bare module cost follow the methodology proposed by Turton in [36].

A generic cost function is expressed in the form of

$$C_{BEC} = C_P^0 * F_m * F_p \tag{5.7}$$

Or

$$C_{BEC} = C_P^0 * (B_1 + B_2 * F_m * F_p) \tag{5.8}$$

in case of heat exchangers, vessel and pumps, where:

- C_{BEC} is the bare erected cost;
- C_P^0 is the purchasing reference cost, in base condition;
- F_m is the material factor;
- F_p is the pressure factor.

In particular the purchasing cost in base conditions, carbon steel construction and near the ambient pressure, can be evaluated with the following equation:

$$C_P^0 = 10^{K_1 + K_2 * log_{10} A + K_3 * (log_{10} A)^2} \tag{5.9}$$

where:

- K_1, K_2 and K_3 are constant useful to fit the expression to the real cost of the device considered;
- A is a size parameter chosen as reference for the device considered.

Each component is analyzed singularly and the various values used in the formulas are correlated with the publication [36]. Since the purchasing costs make reference to the year 2001 in which we have an average value of the CEPCI index equal to 397, the various costs will be brought back to the year 2022 (CEPCI index = 806.9) [34] through the formula:

$$\frac{C_2}{C_1} = \frac{I_2}{I_1} \tag{5.10}$$

where:

- Subscript "2" refers to the desired time;
- Subscript "1" refers to reference time when the cost is known;
- I refers precisely to the Chemical Engineering Plant Cost Index (CEPCI).

The base cost C_P^0 refers to similar units of different size or capacity, so each component is scaled according to its attribute using the six-tenths rule by attracting the value of 0.6 to the exponent n of the formula

$$C_B = C_A * \left(\frac{S_B}{S_A}\right)^n \tag{5.11}$$

where:

- C is the price of the component;
- Subscript "A" refers to the base case;
- Subscript "B" refers to the real case;
- S represent the attribute chosen for the component

In the following, summary tables are proposed in which the main parameters assumed for the calculation are shown, the size item in the table represents the parameter (attribute) by which the formulas are scaled to discount the cost from the base case to the real case.

Compressor

Size [kW]	K_1	K_2	K_3	F_P	F_M
7.4	2.2897	1.3604	-0.1027	1	3.8

Table 5.3: Main constant and assumption for capital cost estimation for the compressor

Heat Exchangers

Size [m^2]	K_1	K_2	K_3	F_P	F_M	B_1	B_2
Area	2.2897	1.3604	-0.1027	1	3.8	0.96	1.21

Table 5.4: Main constant and assumption for capital cost estimation for the heat exchengers

Since heat exchanger evaluation is based on the exchange area, it must be computed:

$$Size = \frac{\dot{Q}}{U * \Delta T_{ml}} \tag{5.12}$$

where:

- $\dot{Q}$ is the heat exchanged;
- U is overall heat transfer coefficient;

- ΔT_{ml} is the logarithmic mean temperature difference.

Pump

Size [kW]	K_1	K_2	K_3	F_P	F_M	B_1	B_2
3.3892	0.0536	0.1538	1	1	1.89	1.35	

Table 5.5: Main constant and assumption for capital cost estimation for the pump

Reformer
Formula 5.13 was used to calculate the reformer price with reference to [7].

$$INV_{REF} = 400 * \left(\frac{m_{H_2}}{750}\right)^2 \tag{5.13}$$

where m_{H_2} is the mass flow rate of hydrogen [kg/h].

Combustor

Size [m^3]	K_1	K_2	K_3	F_P	F_M	B_1	B_2
Volume	3.5565	0.3776	0.0905	0.508456	3.1	1.49	1.525

Table 5.6: Main constant and assumption for capital cost estimation for combustor

WGS reactors
The water gas shift reactor are considered as pressure vessel operating at 16 bar

Size [m^3]	K_1	K_2	K_3	F_P	F_M	B_1	B_2
Volume	3.5565	0.3776	0.0905	0.508456	3.1	1.49	1.525

Table 5.7: Main constant and assumption for capital cost estimation for WGS reactors

PSA
The cost of the PSA component is assumed to be 0.25 €/Nm^3 of biogas upgraded [37].

Finally, 10% will be added to the total cost of the plant, which includes the price of passive components and all other costs necessary to operate the plant.

The assumptions adopted for the calculation of the EPCC, TPC, TOC cost levels are summarised in the table 5.8, to switch from TOC to TASC, the factor 0.114 is used to take into account both the escalation and the interest rate during construction [31]. Once the investment costs have been calculated, calculations are

EPCC	9% BEC
TPC	20% EPCC
TOC	20.2% TPC
TASC	11.4% TOC

Table 5.8: Main assumption for the cost levels estimation

made on maintenance and operation costs.

Following [38], [39]:

Operation & Maintenance Costs	3% Total CAPEX
Operating (1 part time worker, highly automated plant)	20 €/h
Insurance	1% TPC

Table 5.9: Main assumption for OPEX estimation

Chapter 6

Results

This section presents the results obtained.

6.1 Energy analysis

The results referring to the base case, i.e. production of hydrogen from biogas through the steam reforming process with the reforming temperature set at 900 °C, are presented in tables 6.1, 6.2, 6.3 and 6.4.

- The table 6.1 summarizes the components selected and used in the simulations carried out with the Aspen Plus software; for each component, the function, the reaction taking place in it, the operating parameters and the energy required by the component are highlighted. The components used are common to all the simulations carried out.
- The table 6.2 shows the operating parameters of the various streams that make up the system, with evidence on temperature, pressure, mass flow rate, molar flow rate; the molar composition of the components that make up the stream is also shown.
- The table 6.3 shows how the electricity required by the process is due to the compressor and the pump, the rest of the energy represents thermal energy. E_{total} represents the sum of thermal and electrical energy required to run the system.
- Since the hydrogen production process consists of several steps with different temperatures of operation, when the fluids are cooled, heat can be recovered; table 6.4 shows this result for the process with a reforming temperature of 900 °C.

Unit in Aspen Plus	Module	Function	Reaction / Split fraction	Operating Temperature [°C]	Operating pressure [bar]	Energy required [kW]
Reformer	Requilibrium	Simulate reforming process	$CH_4 + H_2O \rightarrow CO + 3H_2$	900	16	78
HT-WGS	Rstoic	Simulate WGS process	$CO + H_2O \rightarrow CO_2 + H_2$ (75% of fractional conversion)	466	16	0
LT-WGS	Rstoic	Simulate WGS process	$CO + H_2O \rightarrow CO_2 + H_2$ (75% of fractional conversion)	241	15.7	0
Condenser	Flash2	Simulate liquid-vapor separation		38	15.7	0
PSA Unit	Separator2	Simulate hydrogen separation	79% split fraction of H_2	38	15.7	0
Combustor	Rstoic	Simulate combustion process		1178.45	1.01	0
C1	Compr	Simulate stream compression				
HE1-HE7	Heater/Cooler	Simulate temperature change of stream				
P1	Pump	Simulate water pump				
V1	Valve	Simulate pressure change				
MIX1-MIX2	Mixer	Simulate mixture of stream				

Table 6.1: Unit, module, function, reaction, split fraction, specification used in Aspen Plus, and Energy required by principal component

Stream	T(°C)	P(bar)	Mass Flowrate (kg/h)	Molar Flowrate (kmol/h)	Molar Composition (%)						
					CH_4	CO_2	H_2O	CO	N_2	O_2	H_2
Biogas	25.00	1.01	59.05	2.16	59.70	40.06	0.00	0.00	0.20	0.04	0.00
Water	25.00	1.01	69.83	3.88	0.00	0.00	100.00	0.00	0.20	0.04	0.00
REF-F	899.67	16.00	128.88	6.04	21.39	14.36	64.16	0.00	0.07	0.01	0.00
REF-P	900.00	16.00	128.88	8.51	0.67	10.19	31.03	14.51	0.05	0.01	43.54
HTS-F	466.26	16.00	128.88	8.51	0.67	10.19	31.03	14.51	0.05	0.01	43.54
HTS-P	350.00	16.00	128.88	8.51	0.67	21.07	20.14	3.63	0.05	0.01	54.42
LTS-P	240.66	15.70	128.88	8.51	0.67	23.79	17.42	0.91	0.05	0.01	57.14
PSA-F	38.00	15.70	101.22	7.01	0.82	28.41	0.52	1.09	0.06	0.01	69.09
TAIL-GAS	37.99	15.65	93.51	3.18	1.79	62.55	1.15	2.41	0.14	0.03	31.94
H_2	37.99	15.65	7.71	3.82	0.00	0.00	0.00	0.00	0.00	0.00	0.00
COM-F	250.00	1.01	274.93	9.17	0.62	21.71	0.40	0.84	27.57	37.77	11.09
FLUE-GAS	200.00	1.01	274.93	8.62	0.00	24.64	13.54	0.00	29.32	32.50	0.00

Table 6.2: Main stream parameters for the H_2-Reforming process at 900 °C

	Component energy needs [kW]	
1	Biogas compressor (electricity)	7.437
2	Biogas heating for reforming reaction	22
3	Water pump (electricity)	0.03
4	Heating and evaporation of water to produce STEAM1	83
5	Endothermal reaction of methane reforming	78
6	Heating of tail gas and air to feed combustion unit	19
7	Heating of tail gas for recycling	0
8	Total thermal energy consumption (8=2+4+5+6+7)	202
9	Total energy consumption (E_{total}),(9=1+3+8)	209.467

Table 6.3: Energy needs of different unit of the global process of hydrogen production at reforming temperature of 900 °C

Recoverable energy form process (cooling) [kW]	
Cooling of syngas form reformer outlet	47
Cooling of syngas form HTWGS outlet	21
Cooling of syngas form LTWGS outlet	34
Heat from tail gas combustion	92
Total recoverable heat	194

Table 6.4: Recoverable energy in the global process of hydrogen production at reforming temperature of 900 °C

Mass flowrate at the inlet of the units [kg/h]						
Unit	Component	Reforming Temperature				
		900°C	850°C	800°C	750°C	700°C
Reforming	Biogas	59.05	59.05	59.05	59.05	59.05
	H_2O	70	70	70	70	70
	O_2	0.03	0.03	0.03	0.03	0.03
	Syngas	129	129	129	129	129
HTWGS	H_2O	47.6	48.8	51.1	54.3	57.78
LTWGS	Syngas	129	129	129	129	129
PSA	Product of LTWGS	129	129	129	129	129
Air	For Mix 2	181	200	232	278	328
Q_{H_2}	kg/h	8	7	6	5	4

Table 6.5: Mass flowrate of components ate the inlet of each unit of the global process of hydrogen production at reforming temperature of 900 °C, 850 °C, 800 °C, 750 °C, and 700 °C

These results analysed in the table 6.5 for the base case of hydrogen production with a reforming temperature of 900 °C change in subsequent simulations with reforming temperatures of 850 °C, 800 °C, 750 °C, and 700 °C, respectively. Based on this, the table summarizes the main results obtained. The layout of the power plant (Figure 5.3) remains unchanged, as do the components used; what changes are the reforming temperature and the input data, which, as mentioned above, are automatically updated thanks to the model settings in Aspen Plus. In order to complete the analysis and in particular to calculate the $Q_{Hot_{min}}$ a term contained in Eq. 5.5, it becomes essential to conduct the Pinch Analysis for each power plant layout proposed in this study.

Unit	Compound	900[°C]	850[°C]	800[°C]	750[°C]	750[°C]
Reforming	CH_4	0.214	0.214	0.214	0.214	0.214
	CO_2	0.144	0.144	0.144	0.144	0.144
	H_2O	0.642	0.642	0.642	0.642	0.642
	CO	0.000	0.000	0.000	0.000	0.000
	N_2	0.001	0.001	0.001	0.001	0.001
	O_2	0.000	0.000	0.000	0.000	0.000
	H_2	0.000	0.000	0.000	0.000	0.000
HTWGS	CH_4	0.007	0.015	0.031	0.055	0.085
	CO_2	0.102	0.104	0.107	0.112	0.118
	H_2O	0.310	0.324	0.349	0.388	0.435
	CO	0.145	0.139	0.128	0.111	0.091
	N_2	0.001	0.001	0.001	0.001	0.001
	O_2	0.000	0.000	0.000	0.000	0.000
	H_2	0.435	0.417	0.384	0.334	0.272
LTWGS	CH_4	0.007	0.015	0.031	0.055	0.085
	CO_2	0.211	0.208	0.203	0.195	0.186
	H_2O	0.202	0.220	0.254	0.304	0.367
	CO	0.036	0.035	0.032	0.028	0.023
	N_2	0.001	0.001	0.001	0.001	0.001
	O_2	0.000	0.000	0.000	0.000	0.000
	H_2	0.544	0.522	0.480	0.417	0.3402
PSA	CH_4	0.008	0.019	0.041	0.078	0.125
	CO_2	0.284	0.286	0.289	0.295	0.788
	H_2O	0.005	0.005	0.005	0.005	0.006
	CO	0.011	0.011	0.010	0.010	0.014
	N_2	0.001	0.001	0.001	0.001	0.001
	O_2	0.000	0.000	0.000	0.000	0.000
	H_2	0.691	0.679	0.654	0.612	0.066
Combustor	CH_4	0.006	0.013	0.024	0.036	0.047
	CO_2	0.217	0.199	0.170	0.137	0.108
	H_2O	0.004	0.004	0.003	0.002	0.002
	CO	0.008	0.007	0.006	0.004	0.003
	N_2	0.276	0.261	0.239	0.214	0.191
	O_2	0.378	0.417	0.478	0.547	0.608
	H_2	0.111	0.099	0.081	0.060	0.041

Table 6.6: Molar composition [%mol] at the inlet of principal unit of the plant at different reforming temperature

Unit	Compound	900[°C]	850[°C]	800[°C]	750[°C]	700[°C]
Reforming	CH_4	0.007	0.015	0.031	0.055	0.0854
	CO_2	0.102	0.104	0.107	0.112	0.118
	H_2O	0.310	0.324	0.349	0.388	0.435
	CO	0.145	0.139	0.128	0.111	0.091
	N_2	0.001	0.001	0.001	0.001	0.001
	O_2	0.000	0.000	0.000	0.000	0.000
	H_2	0.435	0.417	0.384	0.334	0.272
HTWGS	CH_4	0.007	0.015	0.031	0.055	0.085
	CO_2	0.102	0.208	0.203	0.195	0.186
	H_2O	0.310	0.220	0.254	0.304	0.367
	CO	0.145	0.035	0.032	0.028	0.023
	N_2	0.001	0.001	0.001	0.001	0.001
	O_2	0.000	0.000	0.000	0.000	0.000
	H_2	0.435	0.522	0.480	0.417	0.340
LTWGS	CH_4	0.007	0.015	0.031	0.055	0.085
	CO_2	0.238	0.234	0.227	0.216	0.202
	H_2O	0.174	0.194	0.230	0.284	0.350
	CO	0.009	0.009	0.008	0.007	0.006
	N_2	0.001	0.001	0.001	0.001	0.001
	O_2	0.000	0.000	0.000	0.000	0.000
	H_2	0.571	0.548	0.504	0.438	0.357
PSA	CH_4	0.018	0.041	0.084	0.150	0.132
	CO_2	0.625	0.616	0.598	0.570	0.831
	H_2O	0.012	0.011	0.011	0.010	0.006
	CO	0.024	0.023	0.021	0.019	0.0154
	N_2	0.001	0.001	0.001	0.002	0.002
	O_2	0.000	0.000	0.000	0.000	0.000
	H_2	0.319	0.307	0.284	0.249	0.015
Combustor	CH_4	0.000	0.000	0.000	0.000	0.000
	CO_2	0.246	0.231	0.209	0.184	0.162
	H_2O	0.135	0.136	0.137	0.139	0.1402
	CO	0.000	0.000	0.000	0.000	0.000
	N_2	0.293	0.276	0.250	0.221	0.195
	O_2	0.325	0.356	0.404	0.457	0.503
	H_2	0.000	0.000	0.000	0.000	0.000

Table 6.7: Molar composition [%mol] at the outlet of principal unit of the plant at different reforming temperature

Analysing the molar composition at the inlet and outlet of the main components at the Table 6.6 and 6.7, it can be seen that the molar composition of CH_4 at the reformer outlet decreases as the temperature decreases, showing that there is less methane conversion, which will then affect the final hydrogen production. The same reasoning applies to the CO at the outlet of the PSA.

	Component energy needs [kW] @ different reforming temperature [°C]	900[°C]	850[°C]	800[°C]	750[°C]	700[°C]
1	Biogas compressor (electricity)	7.437	7.437	7.437	7.437	7.437
2	Biogas heating for reforming reaction	22	19	17	15	13
3	Water pump (electricity)	0.03	0.03	0.03	0.03	0.03
4	Heating and evaporation of water to produce STEAM1	83	81	79	76	74
5	Endothermal reaction of methane reforming	78	73	65	54	42
6	Heating of tail gas and air to feed combustion unit	19	20	21	24	26
7	Heating of tail gas for recycling	0	0	0	0	0
8	Total thermal energy consumption (8=2+4+5+6+7)	202	193	182	169	155
9	Total energy consumption (E_{total}) (9=1+3+8)	209.5	200.5	189.5	176.5	162.5

Table 6.8: Energy needs of different unit of the global process of hydrogen production at reforming temperature of 900 °C, 850 °C, 800 °C, 750 °C, and 700 °C

The table 6.8 summarizes the results obtained for each of the processes analysed, highlighting the electrical energy, thermal energy and total energy required to run the plant, showing how the total energy consumed, which is the sum of electrical energy and thermal energy, decreases as the temperature decreases. In relation to this decrease in energy, there will also be a similar trend for plant efficiency and hydrogen production, as these parameters decrease with decreasing reforming temperature.

Recoverable energy from process (cooling) [kW] @ different reforming temperature [°C]	900[°C]	850[°C]	800[°C]	750[°C]	700[°C]
Cooling of syngas form reformer outlet	47	42	38	33	28
Cooling of syngas form HTWGS outlet	21	21	20	18	16
Cooling of syngas form LTWGS outlet	34	35	37	41	44
Heat from tail gas combustion	92	103	124	153	184
Total recoverable heat kW	194	201	219	245	272

Table 6.9: Energy needs of different unit of the global process of hydrogen production at reforming temperature of 900 °C, 850 °C, 800 °C, 750 °C, and 700 °C

The table 6.9 shows how the energy required for fluid cooling, which can be recovered as heat, increases as the temperature decreases, especially in relation to consumption due to tail gas cooling

Hydrogen production from biogas with a reforming temperature of 900 °C

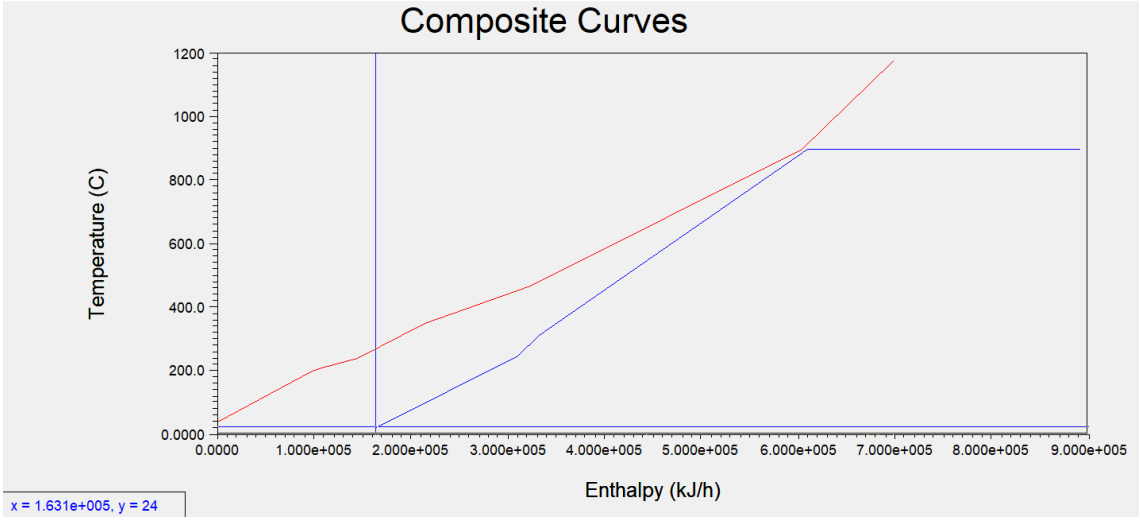

(a)

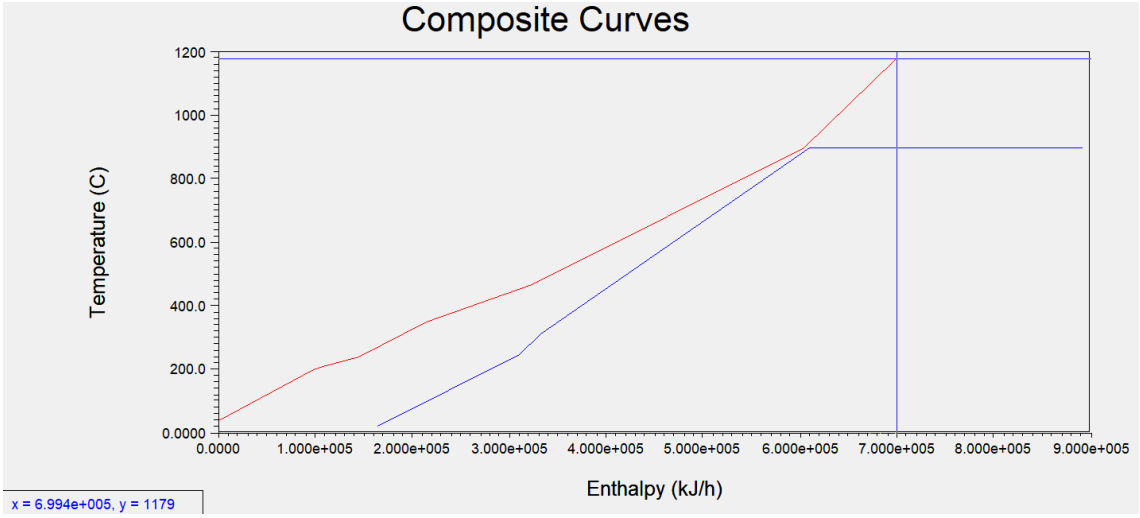

(b)

Figure 6.1: Composite curves for the hydrogen production process with a reforming temperature of 900 °C showing the two points required to determine the recoverable heat energy

Analysis of the results shows that $Q_c = 45.8\text{kW}$ and $Q_h = 53.8\text{kW}$.
And the recoverable heat, equal to the difference between the enthalpy point

highlighted in figure 6.1b and the one highlighted in figure 6.1a is $Q_{rec} = 149.6\text{kW}$.

Hydrogen production from biogas with a reforming temperature of 850 °C

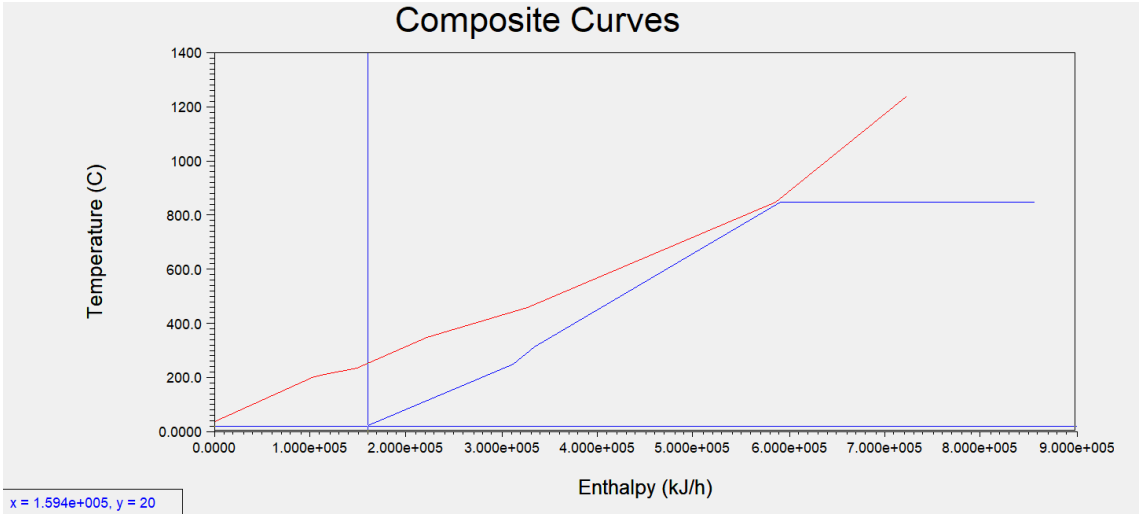

(a)

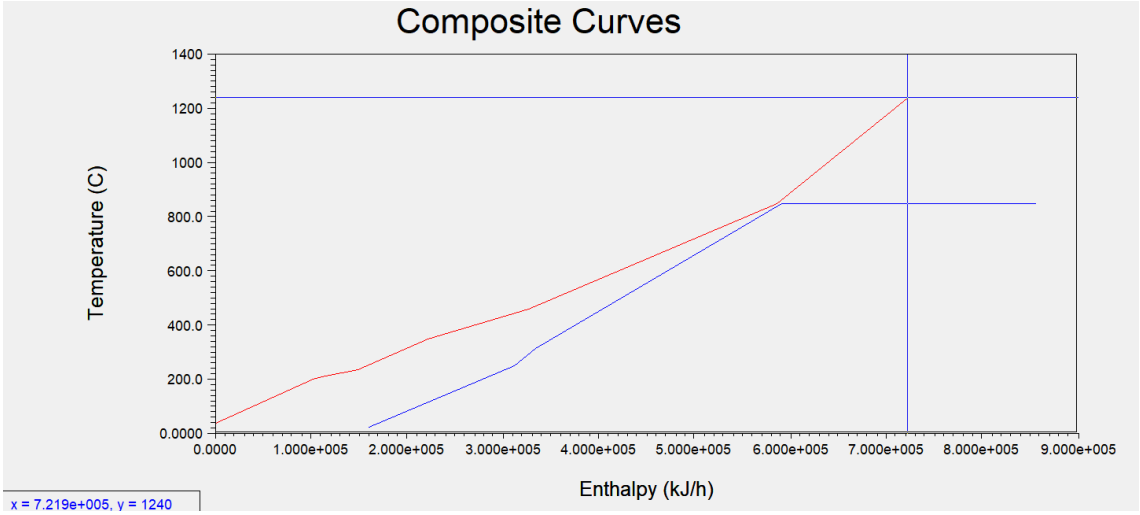

(b)

Figure 6.2: Composite curves for the hydrogen production process with a reforming temperature of 850 °C showing the two points required to determine the recoverable heat energy

Analysis of the results shows that $Q_c = 44.5\text{kW}$ and $Q_h = 36.5\text{kW}$.

And the recoverable heat, equal to the difference between the enthalpy point highlighted in figure 6.2b and the one highlighted in figure 6.2a is $Q_{rec} = 156.3\text{kW}$.

Hydrogen production from biogas with a reforming temperature of 800 °C

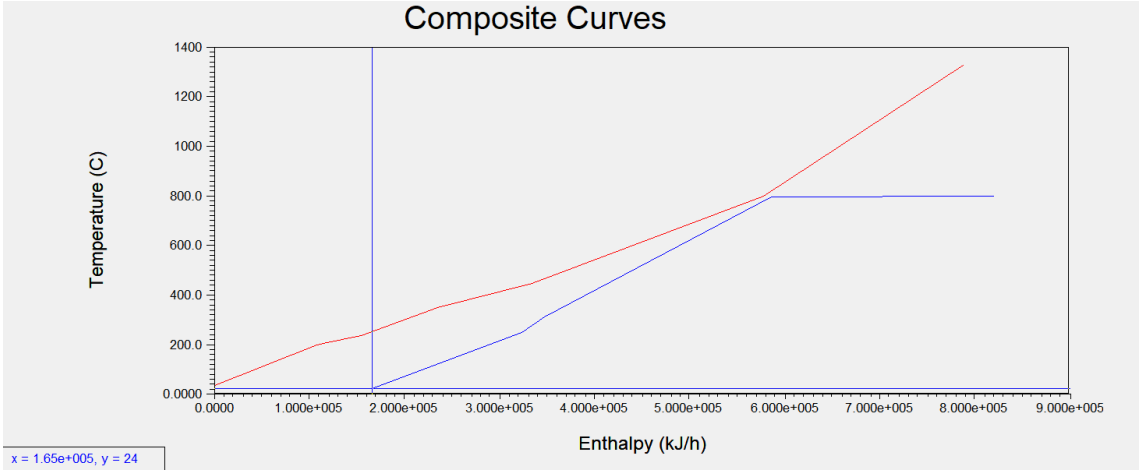

(a)

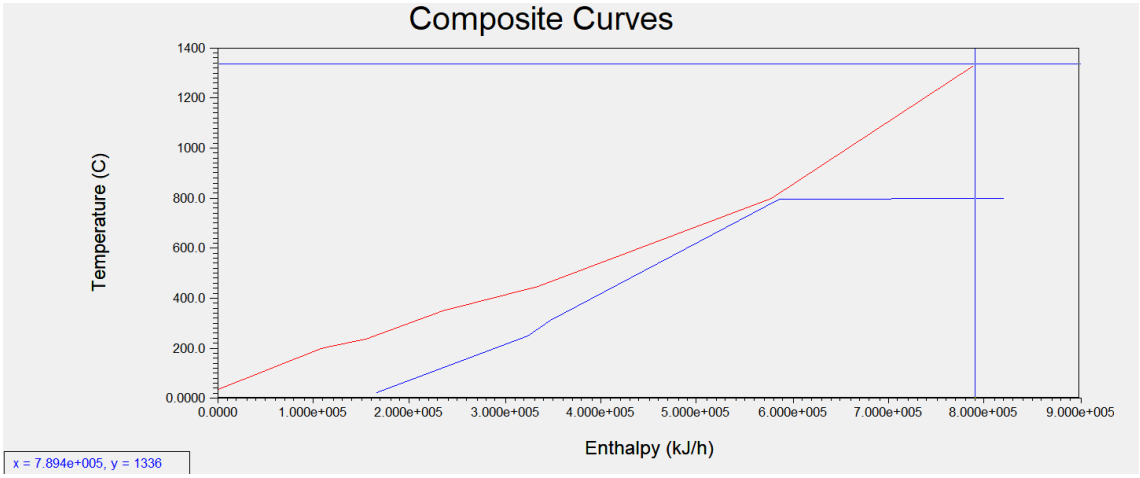

(b)

Figure 6.3: Composite curves for the hydrogen production process with a reforming temperature of 800 °C showing the two points required to determine the recoverable heat energy

Analysis of the results shows that $Q_c = 46\text{kW}$ and $Q_h = 9\text{kW}$.

And the recoverable heat, equal to the difference between the enthalpy point highlighted in figure 6.3b and the one highlighted in figure 6.3a is $Q_{rec} = 173.4$kW. Following the same procedure methodology for processes with reforming temperatures of 750 °C and 700 °C, the results are proposed directly.

Hydrogen production from biogas with a reforming temperature of 750 °C

Analysis of the results shows that $Q_c = 76$kW and $Q_h = 0$kW and the recoverable heat is $Q_{rec} = 169.8$kW.

Hydrogen production from biogas with a reforming temperature of 700 °C

Analysis of the results shows that $Q_c = 117$kW and $Q_h = 0$kW and the recoverable heat is $Q_{rec} = 155.1$kW.

At this point, thanks to the results obtained from the Pinch Analysis through which it was possible to calculate the $Q_{h_{min}}$ term in equation 5.5, it is possible to calculate, for each process, the energetic yield of the global hydrogen production process.

All the results are available and they are summarized on Table 6.10.

Result with PINCH Analysis @ different reforming temperature	900[°C]	850[°C]	800[°C]	750[°C]	700[°C]
Total energy consumption [kW]	209.5	200.5	189.5	176.5	162.5
Total cold flux [kW]	194	201	219	245	272
Total hot flux [kW]	202	193	182	169	155
Total recoverable heat [kW]	149.6	156.3	173.4	169.8	155.1
$Q_{H_{min}}$ [kW]	53.8	36.5	9.0	0.0	0.0
Q_c [kW]	45.8	44.5	46	76	117
$P_{LHV_{biogas}}$ [kW]	287.0	287.0	287.0	287.0	287.0
$P_{LHV_{H_2}}$ [kW]	266.7	233.3	200.0	166.7	133.3
m_{H_2} [kg/h]	8.0	7.0	6.0	5.0	4.0
Plant hour of operation [h]	8760	8760	8760	8760	8760
E_{H_2} [kWh/kg]	**26.2**	**28.6**	**31.6**	**35.1**	**40.6**
η - Energy yield of the global hydrogen production process [%]	**76.6**	**70.5**	**65.9**	**56.6**	**45.3**

Table 6.10: Synthesis of PINCH analysis, energy to produce a kg of H_2 and energetic yield of the global hydrogen production processes at reforming temperature of 900 °C, 850 °C, 800 °C, 750 °C, and 700 °C

6.2 Results comparison

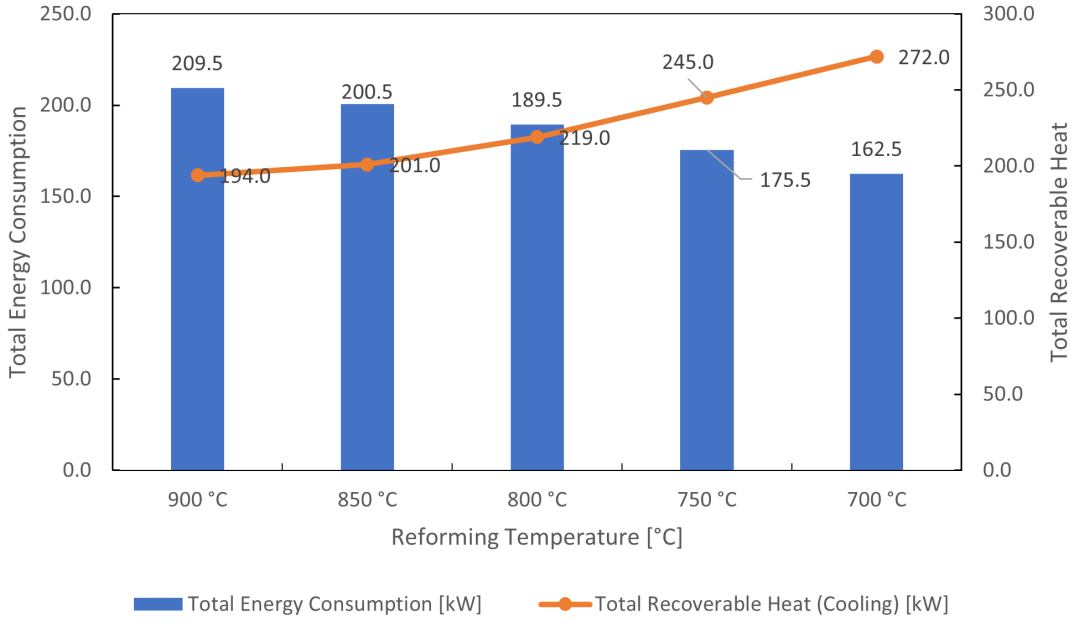

Figure 6.4: Results comparison of different process, Total energy consumption and Total recoverable heat

As can be seen from the last two graphs at Figure 6.7 and 6.8, the simulations with the assumptions made, show how the biogas reforming process is favoured at high temperatures, in particular between 850-900 °C, at these temperatures the highest hydrogen production [kg/h] occur with less energy spent to produce 1 kg of substance. High temperatures, that increase the reaction rate , promote greater conversion of CH_4 in the reformer, so increasing operating temperature is useful, to achieve greater methane conversion and hydrogen production. One must also note that the carbon monoxide content presented a slight increase with increasing temperature. At the same time, the higher the temperature, the higher is the heat duty, causing energy costs and equipment costs to be bigger. As the temperature decreases, the energy yield decreases. This is due to the fact that the process, as the temperature decreases, needs less energy utility and produces less energy, which is a key factor in calculating the energy yield. In particular, the efficiency in relation to the minimum heat to be supplied from outside, calculated using pinch analysis, was higher than that calculated in relation to the total energy consumed by the process. For processes with reforming temperatures of 750 °C and 700 °C, the balance closes without the need for an external hot source, with sufficient internal heat recovery. It can also be seen that as the temperature decreases, the energy

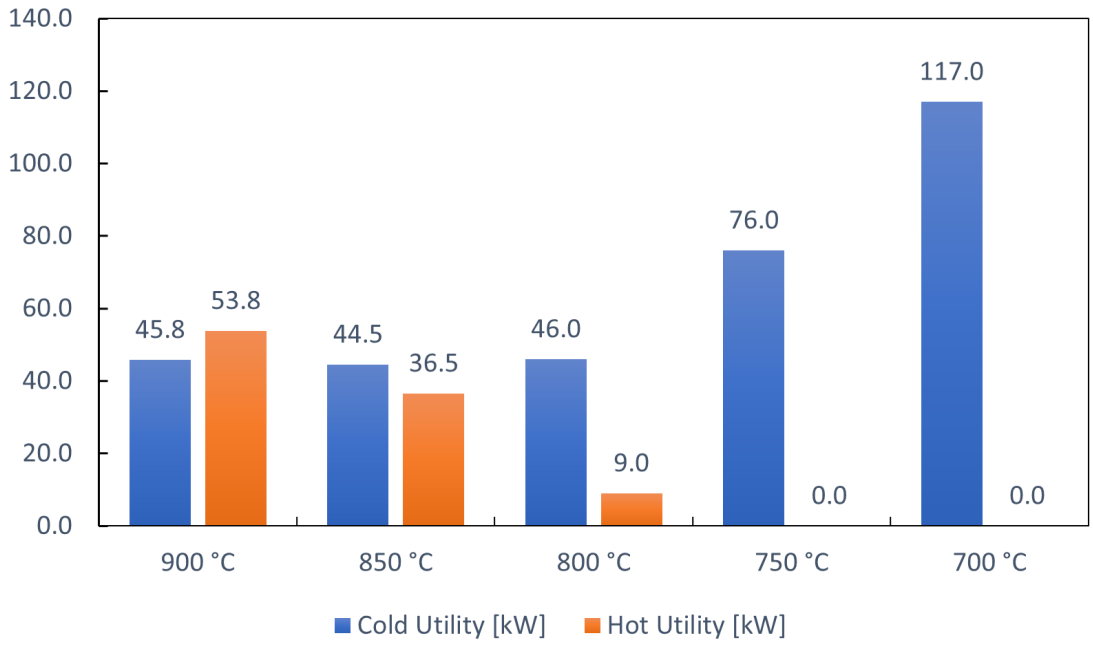

Figure 6.5: Results comparison of different process, Cold Utility and Hot Utility

that can be recovered from the process increases, because there is an increase in the cold flow, mainly due to the cooler at the outlet of the combustor, which will require more energy due to the increase in the temperature of the combustion products. The decrease in temperature also corresponding to a decrease of H_2 production, also equals a decrease in total energy consumption. Finally, with regard to the energy recoverable from the process, pinch analysis shows that it is higher for the process conducted at a reforming temperature of 800 °C.

As far as PSA is concerned, this operates under approximately isothermal conditions, which is why the hydrogen recovery capacity is related to the difference between the supply pressure, which is high, and the regeneration pressure, which is low, of the isotherm [40].

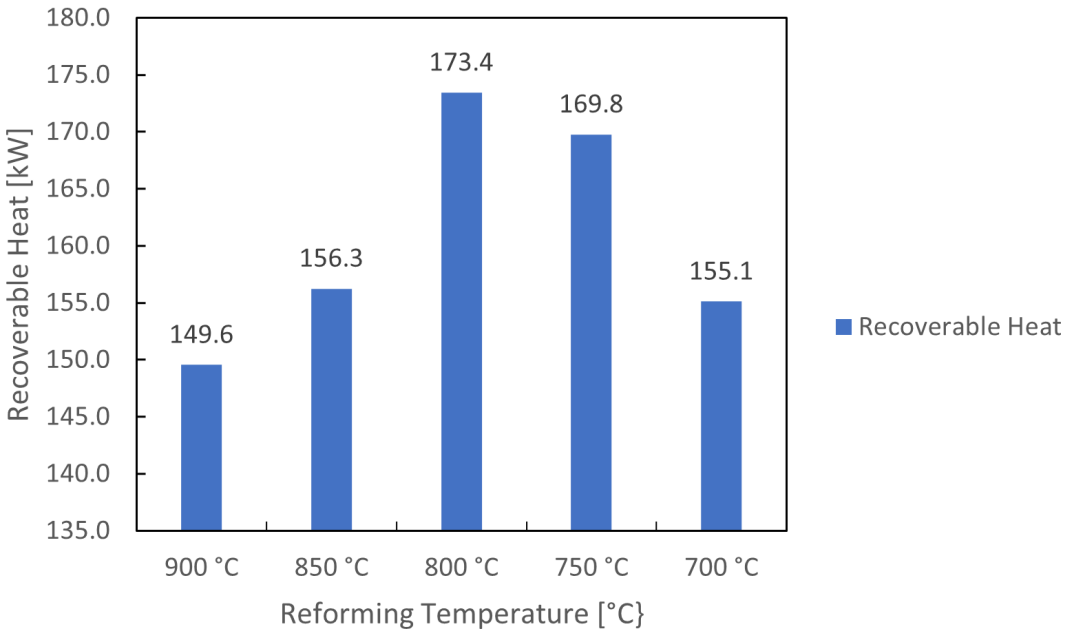

Figure 6.6: Results comparison of different process, Recoverable heat from Pinch Analysis

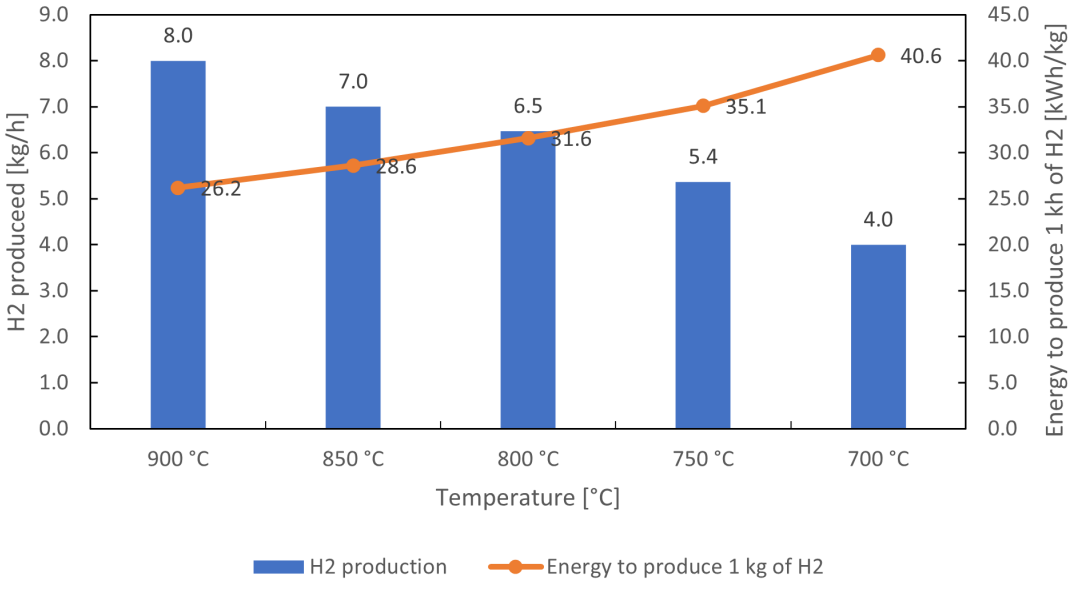

Figure 6.7: Results comparison of different process, H_2 produced and Energy consumed to produce 1 kg of H_2

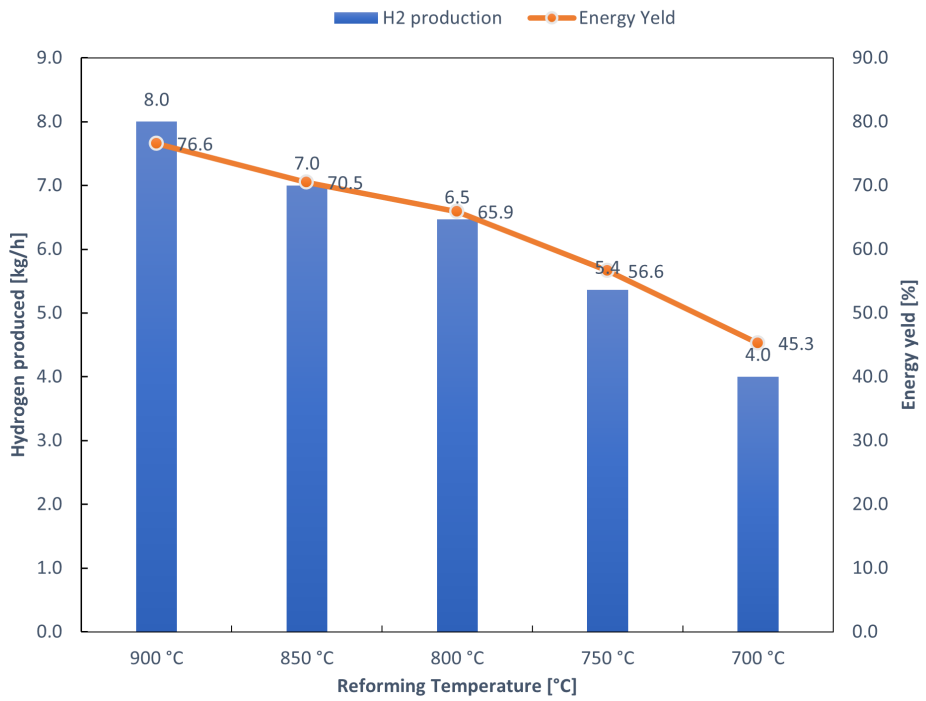

Figure 6.8: Results comparison of different process, H_2 produced and Energy Yield

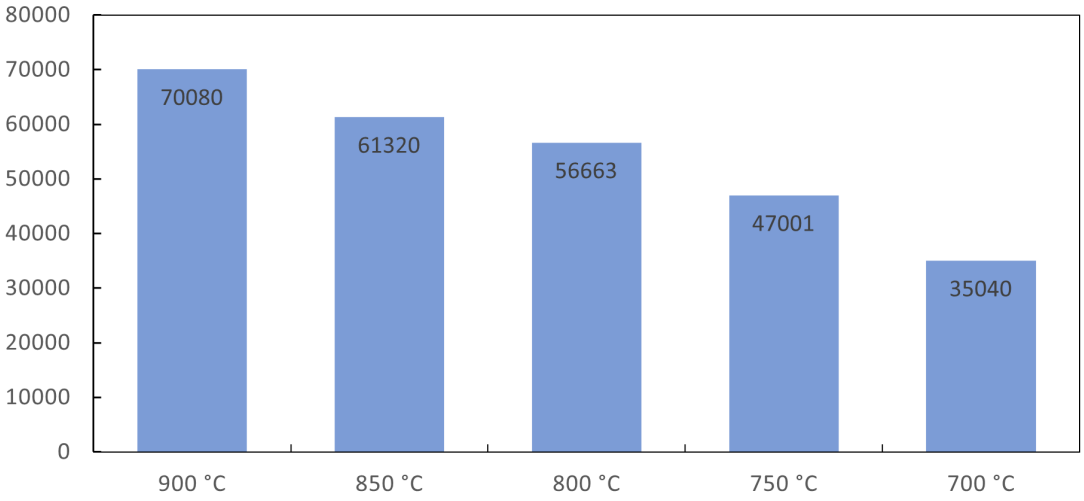

Figure 6.9: Results comparison of different process,H_2 produced in one year of plant operation

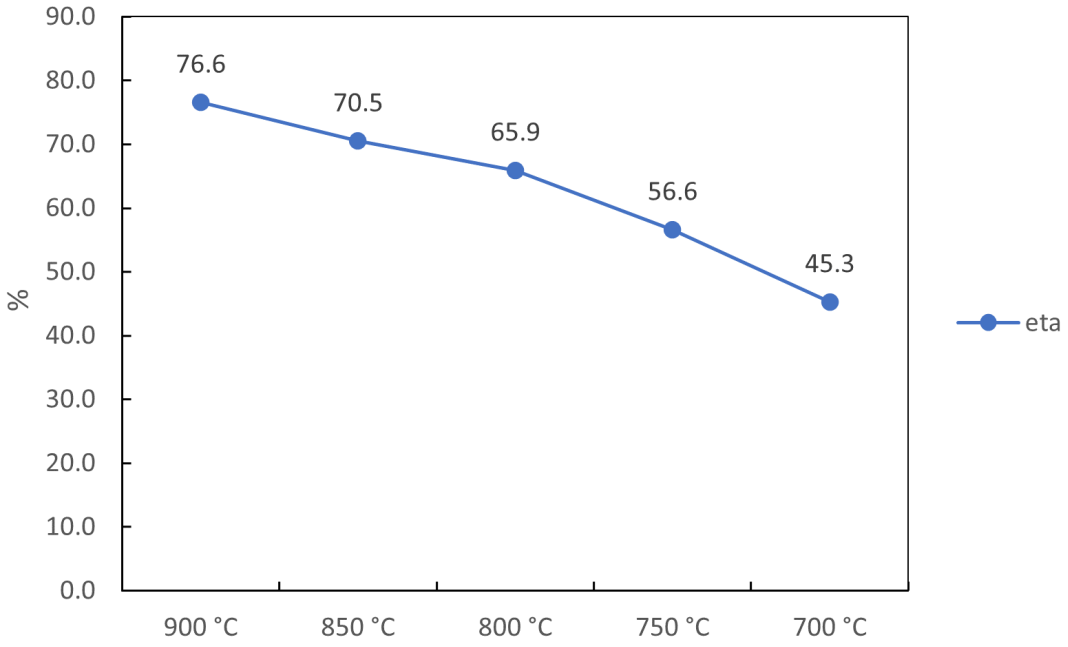

Figure 6.10: Energy efficiency

6.3 Optimization of the heat exchanger network

The results obtained are shown below, in particular a network is proposed for processes at 900 °C, 850 °C, 800 °C, 750 °C, and 700 °C

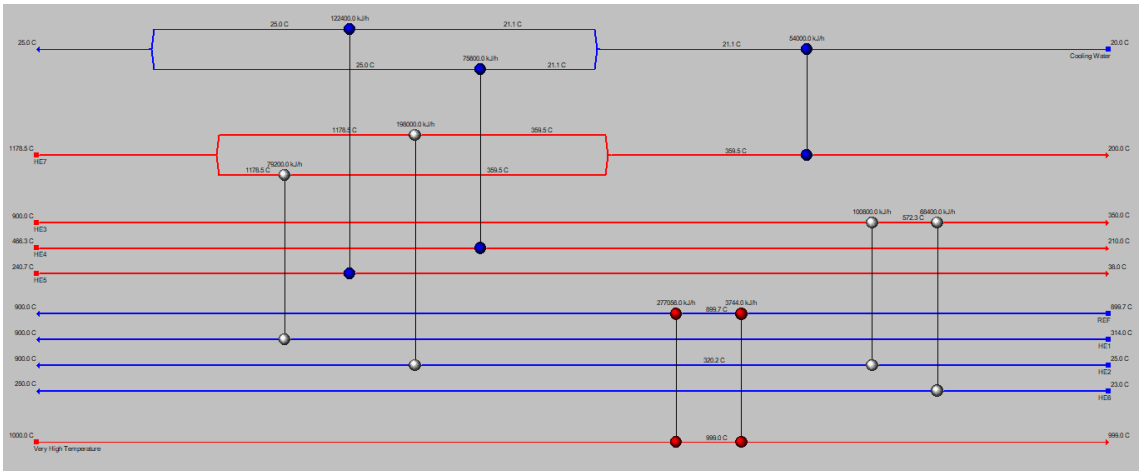

Figure 6.11: Heat exchanger network design for H_2 reforming at 900 °C

Network performance @ 900 °C	
	HEN
Heating [kW]	78
Cooling [kW]	70
Number of unit	9
Number of shell	20
Total Area [m^2]	22.9

Table 6.11: Network performance @ 900 °C

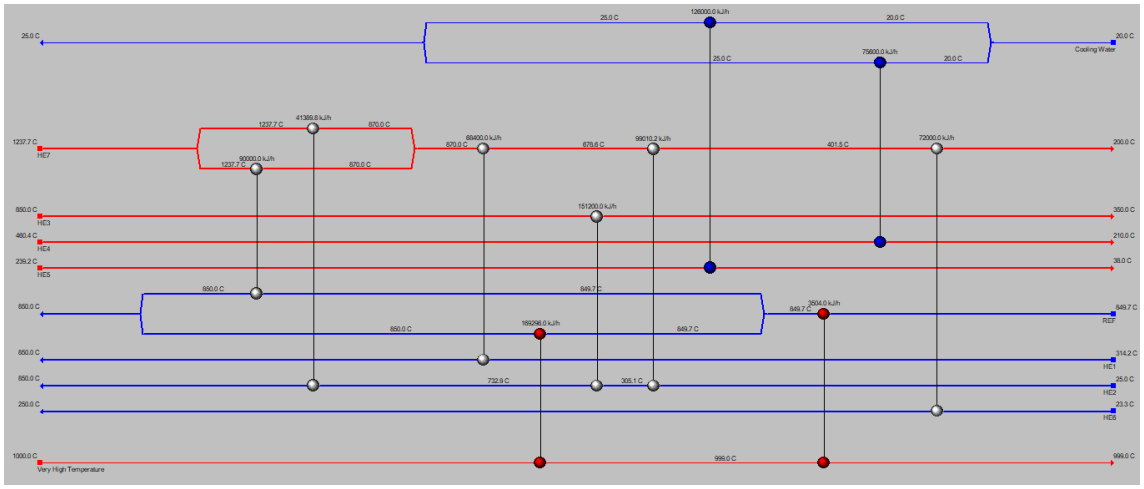

Figure 6.12: Heat exchanger network design for H_2 reforming at 850 °C

Network performance @ 850 °C	
	HEN
Heating [kW]	48
Cooling [kW]	56
Number of unit	10
Number of shell	23
Total Area [m^2]	21.1

Table 6.12: Network performance @ 850 °C

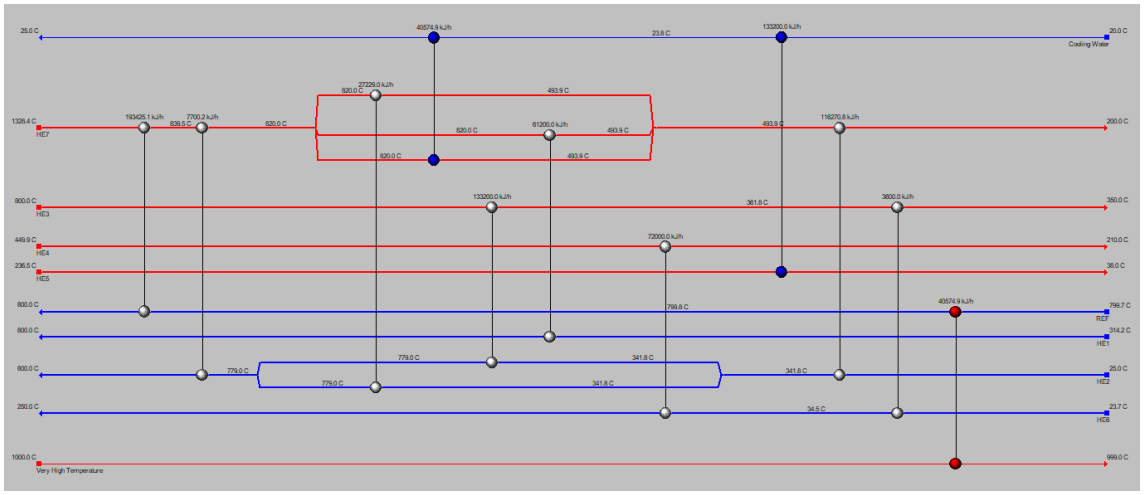

Figure 6.13: Heat exchanger network design for H_2 reforming at 800 °C

Network performance @ 800 °C	
	HEN
Heating [kW]	11
Cooling [kW]	48
Number of unit	11
Number of shell	45
Total Area [m^2]	37.4

Table 6.13: Network performance @ 800 °C

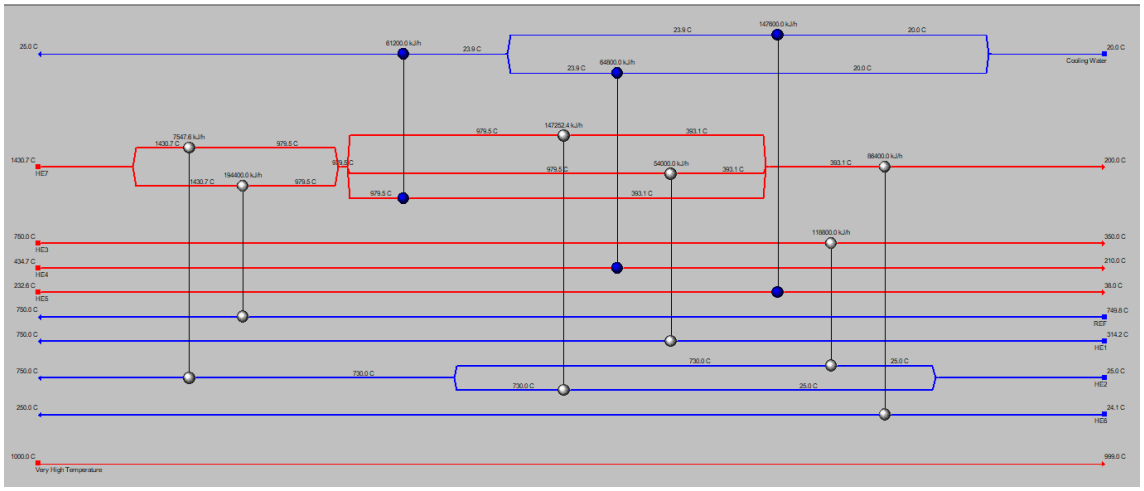

Figure 6.14: Heat exchanger network design for H_2 reforming at 750 °C

Network performance @ 750 °C	
	HEN
Heating [kW]	0
Cooling [kW]	76
Number of unit	9
Number of shell	20
Total Area [m^2]	13.3

Table 6.14: Network performance @ 750 °C

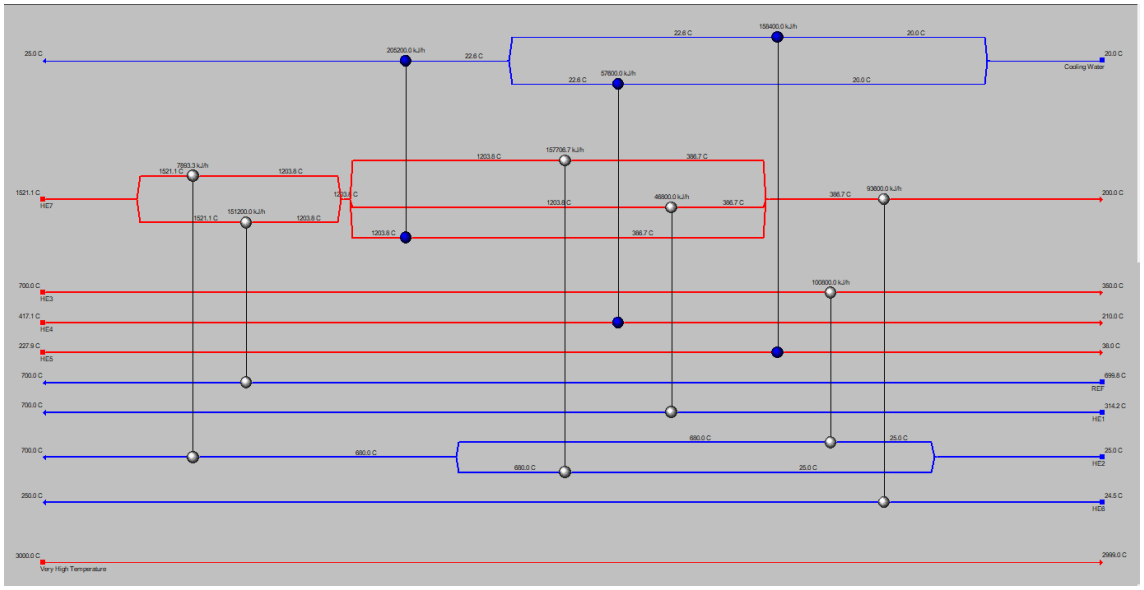

Figure 6.15: Heat exchanger network design for H_2 reforming at 700 °C

Network performance @ 700 °C	
	HEN
Heating [kW]	0
Cooling [kW]	117
Number of unit	9
Number of shell	18
Total Area [m^2]	11.7

Table 6.15: Network performance @ 700 °C

From the results obtained thanks to the Aspen Energy Analyzer V10 software, following the use of the *"Recommended design"* setting, a network of heat exchangers was chosen for each process analyzed, in particular the choice of design was based on having the minimum number of heat exchangers so as to have a good compromise from the point of view of process efficiencies and in such a way as not to increase the investment cost of the plant by much. The process that requires the minimum number of units (equal to 9) are those with reforming temperature of 900 °C, 750 °C, 700 °C, the largest heat exchanger area is found in the process with reforming temperature of 800 °C for which a number of heat exchangers equal to 11 is needed.

Referring to the base case, with a reforming temperature of 900 °C , a comparison test is carried out between two heat exchanger designs, the first layout being the one proposed in the figure 6.11. The second layout considered consists of a network made of a number of heat exchangers equal to 12 and a heat demand from the outside of 63 kW.

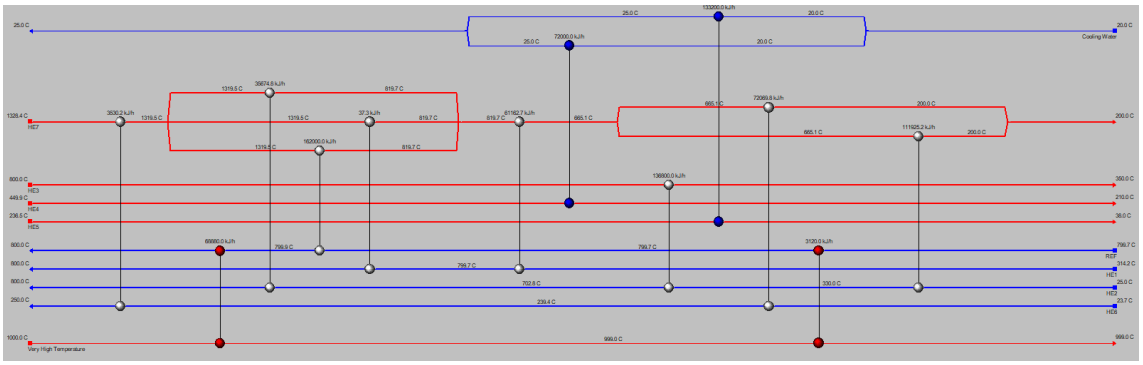

Figure 6.16: Heat exchanger network design for H_2 reforming at 900 °C Design 2

Network performance @ 900 °C Design 2	
	HEN
Heating [kW]	63
Cooling [kW]	55
Number of unit	12
Number of shell	3
Total Area [m^2]	31.6

Table 6.16: Network performance @ 900 °C

A comparison of the resulting efficiencies shows that the one referred to the case with 12 heat exchanger is 5.64% higher than the one with 9 heat exchangers. at the same time in the second layout consisting of 12 heat exchangers, the total area of the heat exchangers is 31.6 m^2 , thus resulting in an increase in area of 27.5% compared to the previously proposed case.

This increase in efficiency would therefore also result in an increase in investment cost for the process.

6.4 Economic results

First of all, the calculated values of the C_p^0 are given, thus referring to the total assumptions, which will then be scaled with the appropriate factors mentioned in the economic methodology in section 5.3.

Component	C_p^0 [€]
Compressor 1 [COMP 1]	150'027.2
Heat Exchanger 1 [EX1]	46'195.5
Heat Exchanger 2 [EX2]	46'195.5
Heat Exchanger 3 [EX3]	46'195.5
Heat Exchanger 4 [EX4]	46'195.5
Heat Exchanger 5 [EX5]	46'195.5
Heat Exchanger 6 [EX6]	46'195.5
Heat Exchanger 7 [EX7]	46'195.5
Pump	2'450.2
Reformer [REF]	359'854.1
Combustor [COMB]	1'859.5
PSA	198'852
HTWGS	1'859.5
LTWGS	1'859.5

Table 6.17: Base cost of components

	BEC[€]	EPCC[€]	TPC[€]	TOC[€]	TASC[€]
COMP 1	98'831.2	10'7726.0	129'271.1	155'383.9	332'522
HE1	38'092.9	41'140.3	49'368.4	59'340.8	126'989
HE2	70'282.5	75'905.1	91'086.1	109'485.5	234'299
HE3	61'812.9	66'758.0	80'109.6	96'291.7	206'064
HE4	53'093.0	57'340.4	68'808.5	82'707.8	176'995
HE5	37'849.8	40'877.8	49'053.3	58'962.1	126'179
HE6	52'559.6	56'764.3	68'117.2	81'876.9	175'217
HE7	56'350.8	60'858.9	73'030.7	87'782.9	187'855
PUMP	1'888.3	2'039.4	2'447.2	2'941.6	6'295
REF	359'854.1	388'642.4	466'370.9	560'577.8	1'199'636
COMB	2'160.5	2'333.3	2'800.0	3'365.6	7'202
PSA	198'852.0	214'760.2	257'712.2	309'770.1	662'908
HTWGS	3'352.5	3'620.7	4'344.9	5'222.5	11'176
LTWGS	2'895.9	3'127.6	3'753.1	4'511.3	9'654

Table 6.18: Cash flow analysis, from BEC to TASC

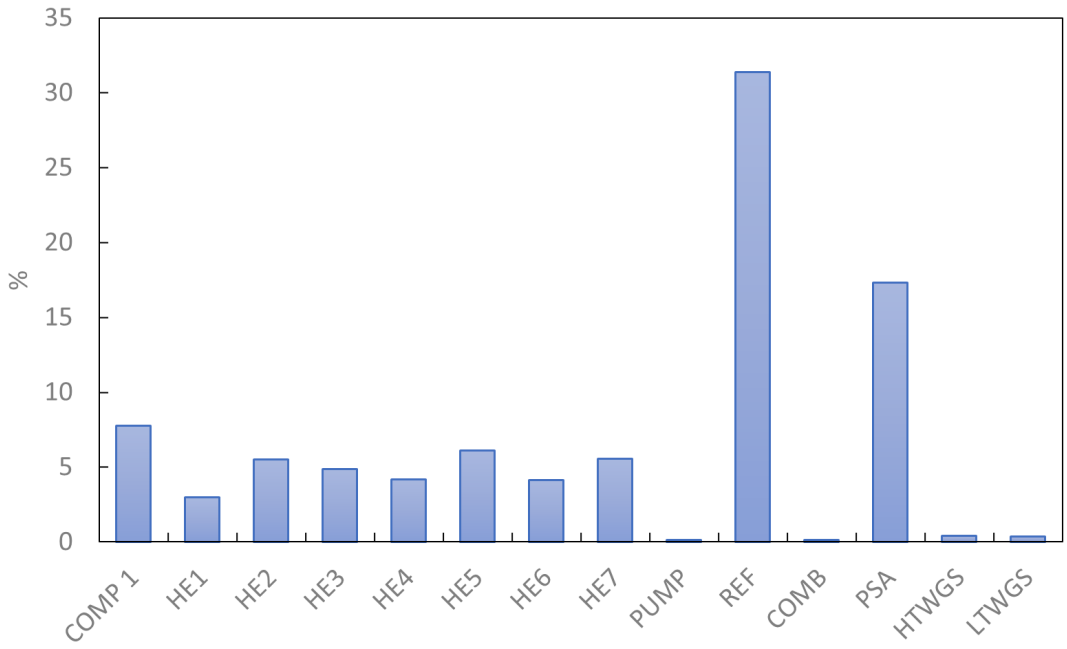

Figure 6.17: Share of total cost of the process

years	CAPEX [€]	OPEX [€]	H_2 (kg/y)	Discounted CAPEX [€]	Discounted OPEX [€]	Discounted H_2 (kg)
1	2076916.5	187477.7	70080	2016423.7	182071.1	68038.8
2		187477.7	70080		176715.7	66057.1
3		187477.7	70080		171568.6	64133.1
4		187477.7	70080		166571.5	62265.2
5		187477.7	70080		161719.9	60451.6
6		187477.7	70080		157009.6	58690.9
7		187477.7	70080		152436.5	56981.5
8		187477.7	70080		147996.6	55321.8
9		187477.7	70080		143686.0	53710.5
10		187477.7	70080		139501.0	52146.1
11		187477.7	70080		135437.8	50627.3
12		187477.7	70080		131493.1	49152.7
13		187477.7	70080		127663.2	47721.1
14		187477.7	70080		123944.8	46331.1
15		187477.7	70080		120334.8	44981.7
16		187477.7	70080		116829.9	43671.5
17		187477.7	70080		113427.1	42399.6
18		187477.7	70080		110123.4	41164.6
19		187477.7	70080		106915.9	39965.6
20		187477.7	70080		103801.8	38801.6
21		187477.7	70080		100778.5	37671.5
22		187477.7	70080		97843.2	36574.2
23		187477.7	70080		94993.4	35509.0
24		187477.7	70080		92226.6	34474.7
25		187477.7	70080		89540.4	33470.6

Table 6.19: Discounted costs and H_2 per year

		LCOH
Tot. discounted costs [€]	Tot. discounted H_2 [kg]	€/kg
5'280'999.9	1'220'313.4	4.33

Table 6.20: LCOH results

From the results obtained, following the various assumptions made, it can be seen that LCOH is comparable with current costs using BSR technology. This cost is slightly higher than that obtained through SMR, but at the same time lower than processes such as photovoltaic-enhanced electrolysis. This technology is now widely used in the literature with studies aimed at evaluating methods to reduce the cost of hydrogen per kg by means of this technology. With reference to [41], it can be seen that the estimated cost of producing hydrogen in a system based on photovoltaics and electrolysis with PEM is $\$18.70/kg_{H_2}$ with a cost projection to 2030 of $\$9.30/kg_{H_2}$. As electrolysis is one of the production methods towards which much attention is now being paid, the work by [42] proposes a cost analysis, related to this technology, showing three different scenarios; in his proposed analysis, the author makes no assumptions about incentives from policies or other financial benefits, focusing on costs associated with capital expenditures and all fixed/variable costs. The technologies that are analyzed are the alkaline electrolyzer, proton exchange membrane, and solid oxide electrolyzer. The renewable electricity considered is derived from solar PV, onshore wind, and offshore wind. In the first scenario the H_2 production plant is directly connected to the grid, thus with a capacity factor of 100 %, but with costs associated with the distribution and transmission of electricity. The results show that the average hydrogen price in the US is \$8.81/kg in 2020 and will decrease to \$5.77/kg in 2050; in Europe it is \$13.11/kg with a projection of \$7.69/kg in 2050. In the second scenario, hydrogen production with connection to a renewable electricity generator is analysed, i.e. operating with CF related to the technology used; in this scenario, no costs are paid for the distribution and transmission of electricity. The results give an average hydrogen price of \$10.61/kg in 2020 in the US, with a projected price of \$5.97/kg in 2050, in Europe an average price of \$19.23/kg in 2020 which is expected to decrease to \$10.2/kg in 2050. In the third scenario, the price of hydrogen produced with a system connected to the transmission grid is analysed, but which only draws energy when energy from renewable sources has to be reduced. In the US, the average cost of hydrogen is \$11.02 /kg in 2020, which will decrease to \$5.92/kg in 2050; in Europe, the average cost of hydrogen will decrease from \$10.85 /kg (2020) to \$6.08/kg (2050).

Chapter 7

Conclusions

Currently, most of the hydrogen produced comes from production methods using fossil fuels, processes that involve the production of pollutants. Hydrogen produced through such systems, which are now mature, has a cost that cannot be reached by 'green' hydrogen production technologies for the time being. The current trend shows that studies are converging towards solutions that will lower the cost of hydrogen produced from renewable sources in the near future. The production of hydrogen from biogas, which leads to clean technology, represents a good opportunity, as it has a production cost that is in the middle of technologies such as SMR and renewable-enhanced electrolysis, such as electrolysis powered by photovoltaic panels. It also represents a technology with a very high CF, capable of operating continuously throughout the year, without the problem of intermittency associated with other types of renewable sources. Power plants exploiting biogas have the potential to be exploited even on a fairly small scale. Hydrogen therefore represents one of the energy vectors that is highly relied upon in Europe and globally to overcome climate challenges and contribute to the decarbonisation process, as H_2 can store and provide large amounts of energy per unit mass without generating and CO_2 emissions during combustion. Based on the experiment analyzed, using Aspen Plus, a study comparing global processes for producing hydrogen from biogas with different reforming temperatures was stuyed.

So the aim of the presented work was to put in evidence that, with the assumption made during the simulations:

- The total energy required by the process decreases as the reforming temperature decreases;
- The hydrogen produced (kg/h) by the process decreases as the reforming temperature decreases;
- The energy required to produce 1 kg of hydrogen increases as the temperature

decreases;

- The efficiency of the process improves with increasing temperature, reaching the maximum value of 78.2% in the process with reforming temperature of 900 °C;
- The minimum number of exchangers to optimize the process is of 9;
- The economic analysis shows that the LCOH of the process with reforming temperature of 900 °C is 4.33 €/kg, showing how this type of technology is competitive to date.

Bibliography

[1] Ministero della transizione ecologica dipartimento per l'energia e il clima, dipartimento per l'energia e il clima direzione generale infrastrutture e sicurezza dei sistemi energetici e geominerari, "La situazione energetica nazionale nel 2020", 2021.

[2] T. E. H. Ambrosetti, "H2 ITALY 2050."

[3] A. Zappi, R. Hernandez, and W. E. Holmes, "A review of hydrogen production from anaerobic digestion," International Journal of Environmental Science and Technology, vol. 18, no. 12. Springer Science and Business Media Deutschland GmbH, pp. 4075–4090, Dec. 01, 2021. doi: 10.1007/s13762-020-03117-w.

[4] A. Tryhuba et al., "Forecasting quantitative risk indicators of investors in projects of biohydrogen production from agricultural raw materials," Processes, vol. 9, no. 2, pp. 1–12, Feb. 2021, doi: 10.3390/pr9020258

[5] K. Chouhan, S. Sinha, S. Kumar, and S. Kumar, "Simulation of steam reforming of biogas in an industrial reformer for hydrogen production," International Journal of Hydrogen Energy, vol. 46, no. 53, pp. 26809–26824, Aug. 2021, doi: 10.1016/j.ijhydene.2021.05.152.

[6] J. v. Karaeva, "Hydrogen production at centralized utilization of agricultural waste," International Journal of Hydrogen Energy, vol. 46, no. 69, pp. 34089–34096, Oct. 2021, doi: 10.1016/j.ijhydene.2021.08.004.

[7] J. G. F. Madeira et al., "Hydrogen production from swine manure biogas via steam reforming of methane (SRM) and water gas shift (WGS): A ecological, technical, and economic analysis," International Journal of Hydrogen Energy, vol. 46, no. 13, pp. 8961–8971, Feb. 2021, doi: 10.1016/j.ijhydene.2021.01.015.

[8] F. Alrashed and U. Zahid, "Comparative analysis of conventional steam methane reforming and PdAu membrane reactor for the hydrogen production," Computers and Chemical Engineering, vol. 154, Nov. 2021, doi: 10.1016/j.compchemeng.2021.107497.

[9] A. Iulianelli et al., "Sustainable H2 generation via steam reforming of biogas in membrane reactors: H2S effects on membrane performance and catalytic activity," International Journal of Hydrogen Energy, vol. 46, no. 57, pp. 29183–29197, Aug. 2021, doi: 10.1016/j.ijhydene.2020.10.038.

[10] M. Ozturk and I. Dincer, "A comprehensive review on power-to-gas with hydrogen options for cleaner applications," International Journal of Hydrogen Energy, vol. 46, no. 62. Elsevier Ltd, pp. 31511–31522, Sep. 08, 2021. doi: 10.1016/j.ijhydene.2021.07.066.

[11] A. I. Osman et al., "Hydrogen production, storage, utilisation and environmental impacts: a review," Environmental Chemistry Letters, vol. 20, no. 1. Springer Science and Business Media Deutschland GmbH, pp. 153–188, Feb. 01, 2022. doi: 10.1007/s10311-021-01322-8.

[12] M. Hermesmann and T. E. Müller, "Green, Turquoise, Blue, or Grey? Environmentally friendly Hydrogen Production in Transforming Energy Systems," Progress in Energy and Combustion Science, vol. 90. Elsevier Ltd, May 01, 2022. doi: 10.1016/j.pecs.2022.100996.

[13] B. Kroposki, J. Levene, K. Harrison, P. K. Sen, and F. Novachek, "Electrolysis: Information and Opportunities for Electric Power Utilities," Golden, CO, Sep. 2006. doi: 10.2172/892998.

[14] Z. Abdin, A. Zafaranloo, A. Rafiee, W. Mérida, W. Lipiński, and K. R. Khalilpour, "Hydrogen as an energy vector," Renewable and Sustainable Energy Reviews, vol. 120. Elsevier Ltd, Mar. 01, 2020. doi: 10.1016/j.rser.2019.109620.

[15] "Office of energy efficiency & renewable energy." https://www.energy.gov/eere/office-energy-efficiency-renewable-energy

[16] N. Gallandat, K. Romanowicz, and A. Züttel, "An Analytical Model for the Electrolyser Performance Derived from Materials Parameters," Journal of Power and Energy Engineering, vol. 05, no. 10, pp. 34–49, 2017, doi: 10.4236/jpee.2017.510003.

[17] "Outlook for biogas and Prospects for organic growth World Energy Outlook Special Report biomethane." https://www.iea.org/reports/outlook-for-biogas-and-biomethane-prospects-for-organic-growth

[18] M. Kaur, "Effect of particle size on enhancement of biogas production from crop residue," Materials Today: Proceedings, 2022, doi: 10.1016/j.matpr.2022.03.292.

[19] T. al Seadi, D. Rutz, R. Janssen, and B. Drosg, "Biomass resources for biogas production," in The Biogas Handbook: Science, Production and Applications, Elsevier Inc., 2013, pp. 19–51. doi: 10.1533/9780857097415.1.19.

[20] R. Campuzano and S. González-Martínez, "Characteristics of the organic fraction of municipal solid waste and methane production: A review," Waste Management, vol. 54. Elsevier Ltd, pp. 3–12, Aug. 01, 2016. doi: 10.1016/j.wasman.2016.05.016.

[21] S. Sarker, A. S. R. Nordgård, J. J. Lamb, and K. M. Lien, "Biogas and Hydrogen," in Hydrogen, Biomass and Bioenergy, Elsevier, 2020, pp. 73–87. doi: 10.1016/b978-0-08-102629-8.00005-0.

[22] S. E. Nayono, "«S. E. Nayono, «Anerobic digestion of organic solid waste for energy production,» 2009".

[23] D. M. Kirk and M. C. Gould, "Bioenergy and anaerobic digestion," in Bioenergy: Biomass to Biofuels and Waste to Energy, Elsevier, 2020, pp. 335–360. doi: 10.1016/B978-0-12-815497-7.00017-8.

[24] E. AgSTAR Program, "Anaerobic Digester/Biogas System Operator Guidebook A Guidebook for Operating Anaerobic Digestion/Biogas Systems on Farms in the United States," 2020. [Online]. Available: www.epa.gov/agstar

[25] "Upgrading del biogas a biometano." http://www.performwater2030.it/info/biogas-upgrading.php#how (accessed Jun. 20, 2022).

[26] " The Anaerobic Digestion Process." https://www.envitechinternational.com/environmental-solutions/biogas-production/ (accessed Jun. 20, 2022).

[27] I. Bioenergy, W. L. Benedetti, A. Pellini, and M. Giannì, "Biogas and biomethane in Italy Deploying biogas and MSW-to-energy GSE GUARANTEES THE SUSTAINABLE DEVELOPMENT OF OUR COUNTRY PROMOTES RENEWABLE SOURCES AND ENERGY EFFICIENCY," 2021.

[28] GSE, «Rapporto statistico 2020 energia da fonti rinnovabili in Italia,» 2022.

[29] T. S. Phan, D. Pham Minh, F. Espitalier, A. Nzihou, and D. Grouset, "Hydrogen production from biogas: Process optimization using ASPEN Plus®," International Journal of Hydrogen Energy, 2022, doi: 10.1016/j.ijhydene.2022.01.100.

[30] B. Linnhoff, "Introduction to Pinch Analysis," in Developments in the Design of Thermal Systems, Cambridge University Press, 2009, pp. 122–138. doi: 10.1017/cbo9780511529528.007.

[31] Netl, "Quality Guidelines for Energy System Studies: Cost Estimation Methodology for NETL Assessments of Power Plant Performance." [Online]. Available: www.netl.doe.gov

[32] Arera, "Prezzi finali dell'energia elettrica per i consumatori industriali - Ue a Area euro," *https://www.arera.it/it/dati/eepcfr2.htm.*

[33] Arera, "Prezzi finali del gas naturale per i consumatori industriali - UE e area Euro," *https://www.arera.it/it/dati/gpcfr2.htm.*

[34] https://www.toweringskills.com/financial-analysis/cost-indices/cepci-2001-to-present

[35] T. Aryandi Gunawan, A. Singlitico, P. Blount, J. G. Carton, and R. F. Monaghan, "Towards techno-economic evaluation of renewable hydrogen production from wind curtailment and injection into the Irish gas network," POLAND, 2012

[36] R. Turton, Analysis, synthesis, and design of chemical processes. Prentice Hall, 2009.

[37] K. Elizabeth and H. Warren, "A techno-economic comparison of biogas upgrading technologies in Europe," 2012.

[38] IEA, "CRITERIA FOR TECHNICAL AND ECONOMIC ASSESSMENT OF PLANTS WITH LOW CO 2 EMISSIONS," 2009. [Online]. Available: www.ieagreen.org.uk

[39] E. Power Research Institute, "TOWARD A COMMON METHOD OF COST ESTIMATION FOR CO 2 CAPTURE AND STORAGE AT FOSSIL FUEL POWER PLANTS," 2000

[40] B. F. Oechsler, J. C. S. Dutra, R. C. P. Bittencourt, and J. C. Pinto, "Simulation and Control of Steam Reforming of Natural Gas - Reactor Temperature Control Using Residual Gas," Industrial and Engineering Chemistry Research, vol. 56, no. 10, pp. 2690–2710, Mar. 2017, doi: 10.1021/acs.iecr.6b03665

[41] J. Hinkley, J. Hayward, R. Mcnaughton, R. Gillespie, M. Watt, and K. Lovegrove, "Cost assessment of hydrogen production from PV and electrolysis Ayako Matsumoto (Mitsui Global Strategic Studies Institute)," 2016.

[42] A. Christensen and A. Co, "Assessment of Hydrogen Production Costs from Electrolysis: United States and Europe,"2020